UPDATE OF THE HL-LHC OPERATIONAL SCENARIOS FOR PROTON OPERATION

S. Antipov, F. Antoniou, R. Appleby, G. Arduini, J. Barranco, P. Baudrenghien, N. Biancacci, C. Bracco, R. Bruce, X. Buffat, R. Calaga, L.R. Carver, M. Crouch, R. De Maria, S. Fartoukh, D. Gamba, M. Giovannozzi, P. Goncalves Jorge, W. Höfle, G. Iadarola, N. Karastathis, A. Lasheen, K. Li, T. Mastoridis, L. Medina, A. Mereghetti, E. Métral, D. Mirarchi, B. Muratori, S. Papadopoulou, Y. Papaphilippou, D. Pellegrini, T. Pieloni, S. Redaelli, G. Rumolo, B. Salvant, E. Shaposhnikova, M. Solfaroli-Camillocci, C. Tambasco, R. Tomás, D. Valuch

The main aim of this document is to have a clearly identified set of beam and machine parameters to be used for numerical simulations and performance assessment. Two scenarios are discussed:

i) Nominal scenario (levelling at a luminosity of 5×10^{34} $cm^{-2}s^{-1}$).
ii) Ultimate scenario (levelling at a luminosity of 7.5×10^{34} $cm^{-2}s^{-1}$).

The value of the luminosity at which levelling is performed is calculated assuming a visible cross-section of 81 mb (corresponding to the inelastic proton-proton cross-section at a center of mass energy of 14 TeV), and the cross-section for the burn-off is conservatively assumed to be 111 mb (corresponding to the total proton-proton cross-section at a center of mass energy of 14 TeV) [1,2]. For both scenarios the main assumptions for the first version of this note [3] were:

i) ATS optics.
ii) New MoGr collimators with a 5 μm Mo coating are installed, in LSS7 only (to replace the secondary collimators). The electrical resistivity of MoGr and Mo is assumed to be 1 μΩm and 0.05 μΩm respectively.
iii) Levelling with β* in IP1&5 and with parallel separation in IP2&8.
iv) Few non-colliding bunches for the experiments (for background studies).
v) Crab Cavities (CCs) are active to provide full compensation of the crossing angle in IP1 and IP5. Continuation of the impedance reduction of the CCs to the required level (and good control of the impedance of new equipment, in particular at large β values).
vi) All the existing circuits should operate at their nominal performance (e.g. non-conformities observed so far should be repaired by Run 4).

An updated version of Ref. [3] is discussed in this note, in particular after four significant modifications [4]

i) CCs will not provide the full compensation of the crossing angle in IP1 and IP5 as their number has been halved [5]: 2 CCs/beam/IP side (i.e. 8 CCs per beam and 16 in total). A crabbing angle of about ±190 μrad will be provided for the nominal voltage of 3.4 MV/cavity for optics version HLLHCV1.3 [6], knowing that 2 CCs on one side of the IP provide the crabbing and 2 CCs on the other side of the IP provide the anti-crabbing.

The work has been done to reduce the impedance of a remaining HOM at 920 MHz by a factor ~ 20 and no significant impedance effect is expected anymore for the nominal and ultimate scenarios discussed in this note [7].

ii) Based on the LHC experience a q-Gaussian distribution [8,9] has been considered to represent the longitudinal distribution and its Full Width at Half Maximum (FWHM) at high energy has to be increased to avoid longitudinal instabilities due to loss of Landau damping [10]. In particular, at high energy the new bunch length is now defined as [9]
   - RMS bunch length (q-Gaussian): 7.6 cm,
   - FWHM bunch length (q-Gaussian): 21.2 cm,

   with q = 3/5 (see also Appendix A). The RMS bunch length of a Gaussian having the same FWHM is 9 cm. It should be noted that the influence of the potential-well distortion (due to the impedance) is rather small, both in the SPS and (HL)-LHC [8,10].

iii) New horizontal and vertical primary collimators is IR7 (2 per beam) are replaced by a new design based on un-coated MoGr. This item has been recently approved by the consolidation project [11]. The long-term plan is to have also the other two primary collimators (i.e. the skew one in IR7 and the one in IR3) replaced by a new design based on un-coated MoGr.

iv) During luminosity levelling, steps of up to 2% are assumed to maximize the integrated luminosity. The main parameter to control luminosity is β^* [12-14]. Optics changes will be performed simultaneously in the two main experiments. However collisions with slightly separated beams can be used to reduce luminosity up to 10% without significantly affecting beam stability. Beam separations can be applied independently in the two main detectors to mitigate luminosity imbalance but also simultaneously to help reducing the number of β^* steps in case optics commissioning time would become an issue.

Several other considerations have also been made, such as

- Optics version 1.3 is now used (called HLLHCV1.3) [6]. The new optics features an optimized phase advance between MKD and TCTs in Points 1 and 5, allowing to reduce the retraction of the TCTs with respect to the TCDQ and TCSP collimators in Point 6. Therefore, the protected aperture can be reduced from 14.6 to 11.9 beam σ [15]. This value of the protected aperture allows to operate the machine down to β^* =15 cm and a full crossing angle of 500 μrad. This assumes that the settings of the TCTH and TCTV are the same despite the aperture margin in Point 5H and Point 1V are larger than Point 5V and Point 1H. Studies on different settings between TCTH and TCTV are ongoing.
- At injection, a β^* of 6 m in Points 1 and 5 is assumed as it gives already plenty of aperture margins. For the ramp and squeeze process LHC is currently limited by the ramp rate of the sextupoles, so starting with a low β^* helps (see also comments later on combined ramp and squeeze).
- At high energy, the β^* reach in Points 1 and 5 for a given choice of flat or round optics depends of the horizontal MKD-TCT1/5 phase advances that are not necessarily the best possible due to optics constraints in Point 6. In case one foresees a swap of the crossing plane between Run 4 and Run 5 as discussed in the TDR [5], there is no best choice for the crossing plane a priori. If one does not foresee the swap of the planes, there is a choice for the

crossing plane in Point 1 and 5 that gives better performance and flexibility depending on the choice of round or flat optics. For round optics, where the aperture bottleneck is in the crossing plane, the best choice is horizontal crossing in Point 1 and vertical crossing in Point 5. For flat optics, where the bottleneck is in the non-crossing plane, the best choice is vertical crossing in Point 1 and horizontal crossing in Point 5. This is because it is in general easier to optimize the MKD-TCT phase advance for Point 1 rather than Point 5. It has also to be noted that any flattening of the round optics with crab cavities implemented by squeezing the β^* in the non-crossing plane will improve performance and having MKD-TCT1/5 phase advance close to ideal values will allow to make full use of the aperture. In the context of this note, for the sake of choosing one scenario, we make the assumption of "H/V crossing in Point 1/5" that gives the best performance for the nominal scenario of round optics with crab cavities. Furthermore we also assume that no swap of the crossing plane will be performed to reduce the accumulated radiation dose in the triplets, as it would require the swap of the CCs.

- The energy deposition studies [16] should be updated taking into account the new conditions for round beams and HLLHCV1.3 optics, i.e. H-crossing in IP1 and V-crossing in IP5, β^* down to 15 cm and constant (for the time being) full crossing angle of 500 μrad.
- New injection working point (due to e-cloud and the high values of chromaticities and Landau octupoles current needed to reach beam stability) used since 2015: (0.27,0.295) instead of (0.28,0.31) [17].
- Laslett tune shifts at injection and linear coupling have to be well corrected to avoid transverse instabilities due to loss of Landau damping [17]. The intensity-dependent tune shifts have been measured in Ref. [18], confirming roughly the predictions [19]. However, it is worth reminding that only a simplified geometry was considered in Ref. [19] and the nominal LHC vertical Laslett tune shift was expected to be $\sim -1.7\times10^{-2}$ at 450 GeV and $\sim -1.1\times10^{-3}$ at 7 TeV (the horizontal tune shift is the same but with opposite sign). As the total beam current will be increased by a factor ~ 2 for HL-LHC, the HL-LHC Laslett tune shifts will be increased by a factor ~ 2 and become $\sim -3.4\times10^{-2}$ at 450 GeV and $\sim -2.2\times10^{-3}$ at 7 TeV (in the vertical plane for the nominal current). Linear coupling ($|C^-|$) should be corrected at the level of 0.002 for injection tunes and 0.001 for collision tunes. In case the tunes would be brought closer to each other, an even better coupling correction would be required as the ratio between the linear coupling strength (i.e. $|C^-|$) and the tune distance to the coupling resonance should be kept constant to avoid a loss of transverse Landau damping [20].
- The bunch length also changed in the SPS with respect to Ref. [3] (taking into account the effect of the impedance and the planned impedance reduction). It is worth reminding that for the momentum spread and the emittance, the values are obtained by computing the trajectory in phase space, taking into account the non-linearities of the RF but without potential well distortion (as evaluated in operation).
- Halo cleaning is expected to be necessary for HL-LHC [21]. Scenarios for providing sufficient transverse Landau damping should be devised without relying on the transverse tails (as it was already the case for the LHC [22, p. 104]) and some margin should be kept to fight against e-cloud. It is thus very important to reduce the impedance of the secondary collimators in LSS7,

as shown in Fig. 1 for the horizontal plane, which is the most critical, just before collision for the ultimate scenario and for a single beam, i.e. without taking into account the interplay between the Landau octupoles and the beam-beam long-range interactions [23]. For the Landau octupoles, the rms tune spread is proportional to the current and the transverse beam emittance: the maximum current of 570 A corresponds to an rms tune spread of 9.3×10^{-5} for the nominal emittance of 2.5 μm at 7 TeV and for the pre-squeeze optics (i.e. without the telescopic part). Neglecting for the moment the beam-beam long-range interactions, the beam (with maximum bunch population and minimum transverse normalized emittance of the beams delivered by the SPS, i.e. 1.7 μm) should be stable for a current in the Landau octupoles (LOF) of ~ 300 A, independently on the sign and even if the transverse tails would be cut down to ~ 3 σ (considering impedance only and no other destabilising effects), for the ultimate scenario at β* = 41 cm. For tighter collimator settings discussed in the past, the situation would be even more critical [24] and it is important to try and disentangle between the different impedance contributors to be able to further improve the beam stability [24]. After the currently approved impedance reduction (with the new collimators in LSS7 and the 2 TCPs), the remaining impedance is almost equally shared between a resistive-wall contribution (mainly due to the TCPs and IR3) and a geometric contribution (with many contributors but without dominant ones) [24].

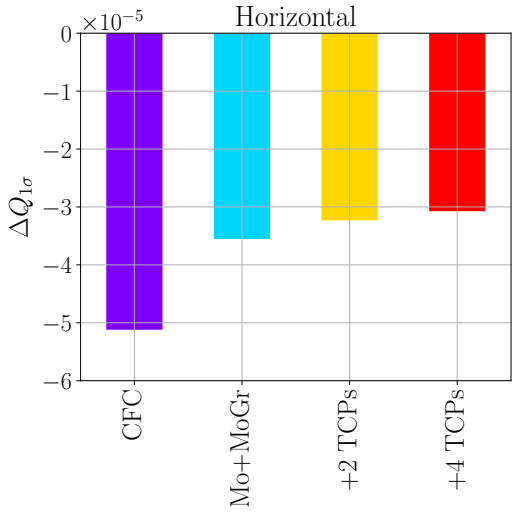

Figure 1: Required rms tune spread to reach single-beam stability for the ultimate scenario at β* = 41 cm and for several impedance models: (i) "CFC" stands for the case with no collimator impedance reduction; (ii) "Mo+MoGr" stands for the case with new MoGr collimators with a 5 μm Mo coating installed in LSS7 only (to replace the secondary collimators); (iii) "+2 TCPs" means that in addition to (ii), 2 TCPs are replaced by a new design based on un-coated MoGr; (iv) "+4 TCPs" means that in addition to (iii), 2 additional TCPs are replaced by a new design based on un-coated MoGr.

The stability limits are constantly being reviewed as a function of the observations made at the LHC: based on the past LHC operational experience, a margin in the Landau octupoles current by a factor at least 2 would be highly desirable, as the machine impedance can only be worse than in the idealistic

model considered above and other destabilizing effects might appear (such as e.g. e-cloud or loss of Landau damping due to linear coupling already observed during Runs 1 and 2). Further studies are ongoing to i) try and continue to reduce the impedance of the main contributors; ii) try and avoid to use the tighter settings of the collimators already at the end of the ramp (but this might generate more beam loss spikes during the ramp); iii) use the ATS telescopic part already during the combined ramp and squeeze to avoid the significant reduction of the stability diagram due to the interplay between the Landau octupoles (with negative sign) and the beam-beam long-range interactions [25]. Indeed, with the chosen sign of the Landau octupoles (see discussion below on the pros and cons), the beam-beam long-range interactions will fight against the Landau octupoles [26], reducing the tune footprint and associated stability diagram [27-29], as depicted in Fig. 2. Figure 2 clearly reveals that without the impedance reduction beam stability cannot be reached in the ultimate scenario (i.e. colliding at β* = 41 cm).

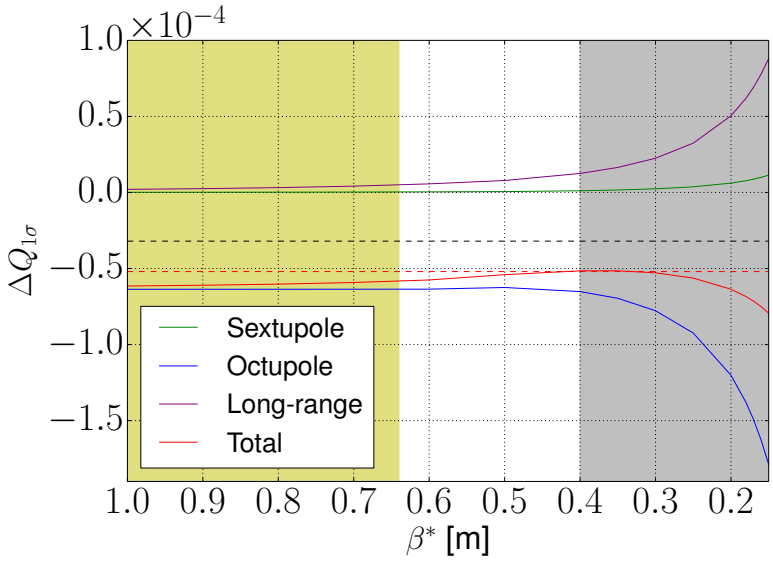

Figure 2: Evolution of the rms tune spread during the betatron squeeze for the most critical BCMS beam in the ultimate scenario (i.e. colliding at β* = 41 cm), taking into account the Landau octupoles (at the maximum current of 570 A but with the negative sign), the beam-beam long-range interactions and the telescopic part of the ATS optics. The red horizontal dashed line corresponds to the required value for single-beam stability without impedance reduction, while the black one corresponds to the case with the low-impedance collimators. Note that in Fig. 2 several assumptions have been made: constant beam impedance, constant beam intensity and no beam-beam head-on collisions (i.e. when the beams are still separated). Therefore it is not valid once in collision (i.e. in the present case below β* = 41 cm) as other mechanisms need to be taken into account.

The collision process (i.e. the collapse of the beam separation) has been studied in detail in the past for previous settings [25] and it is currently being redone with the updated parameters. During the fill (in collision), the bunch intensity will decrease and it will be possible to decrease the Landau octupoles current accordingly, still preserving the beam stability of the non-colliding

bunches. As concerns the colliding bunches in IP1&5, thanks to the beam-beam head-on tune spread providing much more Landau damping than the Landau octupoles, the Landau octupoles current could be significantly reduced (as well as the chromaticities) [25]. Therefore, in stable beams the constraints on the Landau octupoles current and chromaticities should come only from the non-colliding (in IP1&5) bunches. This is why they will be treated separately in the following Tables related to the "stable beams" process. Of course if the experiments are ready to accept non-colliding bunches with lower brightness (as for instance during Run 2), then this constraint disappears.

- As concerns the sign of the Landau octupoles, several considerations need to be taken into account
    - The negative sign of the Landau octupoles provides more Landau damping than the positive one for the single-beam instabilities assuming a Gaussian transverse beam profile (by a factor ~ 1.7 and thanks to the tails) [30]. However, as one should not rely on the tails and a halo cleaning might be necessary, the studies are made assuming a quasi-parabolic distribution (cut at ~ 3.2 σ) and in this case there is no clear preference between positive and negative sign [30]. In fact, the positive sign becomes even a bit better.
    - The negative sign of the Landau octupoles is better for DA considerations [31-42] (see below).
    - However, during the betatron squeeze the beam-beam long-range interactions fight against the Landau octupoles [26], reducing the tune footprint and associated stability diagram [27-29] (see Fig. 2). The possible solutions to overcome this problem are
        - Continue and reduce the transverse impedance to have sufficient margin even in the presence of the reduced stability diagram: either replace other collimators or try and use more relaxed settings until collision, where sufficient stability is provided by the beam-beam head-on tune spread.
        - Collide earlier: the beneficial effect of colliding earlier is clearly seen from Fig. 2.
        - Start the telescopic part of the ATS optics (which increases the β-functions at the locations of the Landau octupoles, increasing the stability diagram) earlier to compensate the reduction coming from the beam-beam long-range interactions and even increase the margin. A trade-off between beam stability and DA would have to be found.
    - An other possibility is to use the positive sign of the Landau octupoles and change the sign of the Landau octupoles in collision. This is predicted to be fine for the colliding bunches (as the tune spread is dominated by the beam-beam head-on) but not for the non-colliding bunches, which should become unstable leading to beam loss and/or significant transverse emittance blow-up.
- Instabilities attributed to e-cloud have been observed in the LHC also in collision, which required increasing the vertical chromaticities to values slightly higher than 20 [43]. However, according to simulations [43], this mechanism should occur for bunch populations below ~ 1×10^{11} p/b and therefore it should not be an issue for HL-LHC [44].

- The destabilising effect of the (resistive) transverse damper for low chromaticities is under study as it could set a limit on the minimum chromaticity to be used [45].
- The effect of space charge was also recently investigated, revealing its beneficial effect on the intensity threshold for both TMCI and Head-Tail instability regimes, below a certain energy [46].
- Combined ramp and squeeze has been tested successfully during Run 2 in the LHC and it is proposed to be implemented in HL-LHC tentatively down to 64 cm (which is the β* at which the collisions will occur for the nominal scenario). This value will be refined when the final squeeze sequence will be validated taking into account the final ramp rate limitation of the HL-LHC circuits and beam-beam considerations. This leads to a reduction of the minimum turn-around time compared to the 180 minutes mentioned in Ref. [5] (see Table 1).

Table 1: Minimum turn-around time.

Phase	**Time [minutes]**
Ramp-down	40
Pre-injection set-up	15
Set-up with beam	15
Nominal injection	30
Prepare ramp	5
Ramp & Squeeze	25
Flat-top	5
Squeeze	0 (nominal) / 5 (ultimate)
Adjust/collide	10
TOTAL	145 (nominal) / 150 (ultimate)

This might require the commissioning of the Main Sextupole and Landau octupole circuits to higher ramp and acceleration rates as compared to the lower ones tested during HWC and operation and/or a revision of the cycle generation process. It should be noted that in the above Table the time for a pre-cycle (30 min) has not been included as the latter is supposed to be performed only sporadically. **Furthermore, it is worth mentioning that with an upgrade of the IR2&8 triplet circuits the ramp-down time could be reduced from 40 min down to 25 min, gaining therefore 15 min**. Moving from the injection working point to the collision working point during the ramp requires a good control of linear coupling, otherwise transverse instabilities due to a loss of Landau damping might arise [20].

- Following the successful commissioning of IR non-linear correctors, it is proposed to operate the non-linear correctors in HL-LHC by ramping their strength to the nominal value linearly during the energy ramp.
- The spacing between PS/SPS trains has been reduced to 200/800 ns following the 2017 operational experience [47,48] and the maximum numbers of bunches per beam and colliding pairs have been updated accordingly as reported in the following Tables. Concerning the BCMS beam, the compatibility of these beam parameters with the protection devices involved in the SPS-LHC transfer still needs to be validated within the LIU project [49].

- Detailed Dynamic Aperture (DA) simulations (successfully benchmarked in the LHC) were performed to optimize the relevant beam parameters [50]. The DA can be improved by reducing both the Landau octupoles current (as shown in Fig. 3(left) for the most critical case of the β* of 15 cm at the end of the fill) and chromaticities, as it was also known from previous simulations and proved experimentally in the LHC in 2015 beam-beam long-range experiments [38]. In this plot, the luminosity of LHCb is at 2×10^{33} cm^{-2} s^{-1}, β* = 3m with 1.25 σ of beam-beam head-on half-separation separation (for the present baseline layout including Main Sextupoles in cell 10, called MS10). A half crossing angle of 250 μrad looks feasible with Landau octupoles at ~ - 100 A (which is considered to be sufficient to stabilize the colliding bunches taken into account the enhancement of the β -function at the octupoles – by a factor 3.333 at β*=15 cm - in the sectors participating to the telescopic squeeze, i.e. in only half of the sectors). It might be possible to gain some more margins by reducing the chromaticities to 10 or less and/or optimizing the working point. If the Landau octupoles current cannot be reduced, a solution can be found by optimizing the working point, as can be seen in Fig. 3(right).

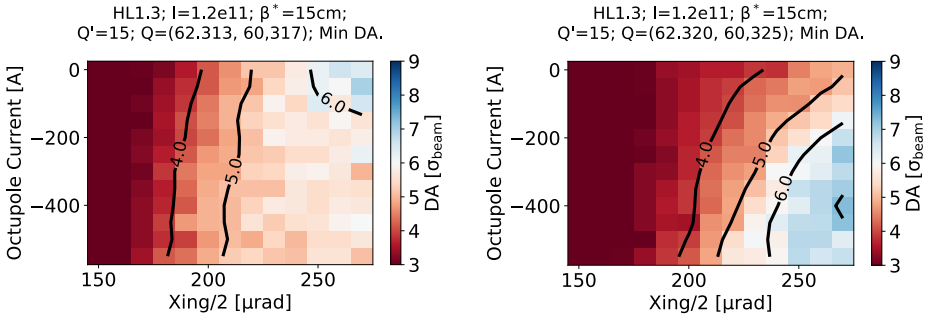

Figure 3: DA simulations for the most critical case of β* = 15 cm at the end of the fill: (left) a half crossing angle of 250 μrad looks feasible only if the Landau octupoles current can be reduced down to ~ - 100 A; (right) if the Landau octupoles current cannot be reduced, a solution is found by optimizing the working point.

- In case limitations from e-cloud effects are encountered (e.g. heat loads, instabilities) the 8b+4e filling pattern [51] will be employed to mitigate the e-cloud formation at the expense of a reduction in number of bunches. With this configuration, a maximum of 1972 bunches can be stored in the LHC [52]. The injected bunch population will be the same as for the baseline scenario (2.3×10^{11} p/b), and the normalized transverse emittance will be 1.7 μm. In order to adapt the heat loads on the beam screens to the available cooling capacity while maximizing the number of colliding bunches, 8b+4e trains can be mixed with standard trains in the same filling scheme. This possibility was successfully tested in MD during 2016 [53].
- CCs will be operated with RF ON with strong RF feedback and tune controls at all times. The following settings are considered
  - During filling, ramping or operation with transparent CCs

        - A small cavity field (0.25 MV/CC) is required for the active tuning system.
        - Counter-phasing is used to make the total field invisible to the beam.
        - A strong RF feedback keeps the beam-induced voltage to zero if the beam is off-centred. At injection and with 0.25 MV/CC, a static beam displacement of 2 mm would require 19 kW from the amplifier (out of 40 kW maximum) to compensate for the beam loading (if the displacement is in the most critical direction).
    - Before the collision process
        - Counter-phasing will be driven to zero, CC voltage will be raised to nominal value.
        - Any adiabatic field manipulation is possible by synchronously changing the voltage or phase in each cavity (e.g. when changing the crossing angle or for luminosity levelling).
    - The studies of emittance growth in the presence of the transverse damper (ADT) noise and tune spread should be done throughout the cycle considering the RMS tune spread resulting from the Landau octupoles during the cycle. In collision the tune spread will be dominated by the beam-beam head-on interaction and the RMS tune spread to be considered is 0.17 times the beam-beam tune shift [54]. The noise requirements should be based on a total beam-beam tune shift of ~ 0.02 (as the beam-beam tune shift per IP is ~ 0.01 and IP8 will not collide head-on), and therefore a RMS tune spread of ~ 0.0034. For the current baseline, the maximum acceptable transverse emittance blow-up to avoid less than ~ 1% of luminosity loss is ~ 0.05 μm/h as the CCs should provide an additive (and not multiplicative) source of blow-up [55] (see also Appendix B). To compare to the current situation in the LHC in 2017 with the 8b+4e beam, exactly the same number was obtained for the transverse emittance growth of the colliding bunches in stable beams [56]: ~ 0.05 μm/h for both beams and both planes. Detailed benchmarks to LHC data explain why the weak-strong analytical estimates are used to describe the transverse emittance growth (even if not fully understood yet) [57].
- For the longitudinal beam loading compensation, the half-detuning scheme was used in the LHC between 2008 and 2016. In this scheme, the voltage is kept constant (amplitude and phase) over the turn and the required power from the klystrons to compensate the beam-induced voltage scales with the beam current. At injection, with a voltage per cavity of 1 MV, the half-detuning schemes would require 250 kW per klystron, compatible with their peak power (300 kW). Reducing the voltage per cavity would help to have more margin (e.g. using 0.75 MV per cavity would reduce the required klystron power down to 190 kW). Since 2017, the full-detuning scheme is used [58,59], where the cavity voltage amplitude is kept constant but a phase modulation caused by the beam loading is accepted. In this way, the required power from the klystron is constant and independent of the beam current. Without the full detuning scheme it would not be possible to accelerate the future high-intensity beams without major upgrades of the RF system. The procedure is to use the old scheme (half detuning, i.e. without phase modulation) for the injection process, during which the required voltage is much reduced, as the bunch spacing from SPS is constant, and switch to the new scheme (full

detuning, i.e. with phase modulation) immediately before starting the ramp. With a full machine, the phase modulation is dominated by the length of the so-called abort gap (i.e. the no-beam segment required for the rise-time of the beam dump kicker). The peak-to-peak phase modulation scales linearly with the abort gap length and inversely to the cavity voltage. It is also dependent on the longitudinal bunch profile, so it will change somewhat during physics as the longitudinal profile evolves. The length of the abort gap is 1200 RF buckets, i.e. 3 μs, and the last RF bucket before the abort gap is 34421. On-line estimates of the peak-to-peak RF modulation can be found here: https://lpc.web.cern.ch/cgi-bin/filling_schemes.py.

- The power loss due to synchrotron radiation reaches 34 W per half-cell and per beam at 7 TeV, i.e. it is 0.32 W/m/beam [60].
- In the four experimental insertion regions, a low SEY (Secondary Emission Yield) coating (< 1.1) of the inner triplet beam screens and DS (Dispersion Suppressors) is foreseen in the baseline: in IR1&5, which will be changed (and will be equipped with dedicated cryoplants) and in IR2&8, where the coating will have to be done in-situ. The total length of non-coated parts should be minimized (as much as possible); and as the heat load in IR2 and IR8 will affect the neighboring arcs, it is desirable to have also a low SEY coating of the matching sections (stand-alones) [61]. Amorphous carbon (a-C) performances have to be validated at cryogenics temperature and an in-situ a-C coating of the triplets in Points 2 and 8 is foreseen [62]. The temperature of the new a-C coated shielded beam screens in Points 1 and 5 will be higher than the usual 5-20 K: 60-80 K is currently contemplated [63].
- As concerns the LHC arcs, taking into account the effect of the photoelectrons we can conclude that measurements for the cells with the current lowest heat loads (in S34, S45, S56 and S67) are compatible with a low SEY parameter (corresponding to full surface conditioning, or to SEY ~ 1.25) [64,65]. The measurements for the half-cells with the largest load (in S12 and S81), instead, correspond to SEY ~ 1.35. The priority is therefore to identify and suppress the source of large heat loads in S12, S23, S78 and S81, and to preserve the performance in the other arcs since they are compatible with HL-LHC but there is no much margin available. It is worth reminding that the sectors 23 and 78 will be the weakest even after the HL-LHC new cooling installations [66].
- The beam-beam head-on interactions lead to a maximum β-beating amplitude of ~ 7% (with a beam-beam parameter of $\xi = 0.01$) for LHC and ~ 14% for HL-LHC ($\xi = 0.02$), with a beating at the IP at the level of few percent [67]. The impact of the β-beating on the luminosity has been computed confirming that the effect is at the few percent level for the typical beam-beam parameters. A possible strategy would be to leave the effect uncorrected and recover the loss or gain of luminosity with separations [67,68].
- Several levelling techniques are available [69]:
    - Levelling by transverse offset is operational since Run 1.
    - The crossing angle levelling has been made operational since June 2017.
    - The β* levelling has been tested in MDs. In between the matching points some β-beating and tune shift appear, which are observed as losses, which should be reduced by additional smoothing. As concerns

beam stability, the beam-beam full separation at the IP should remain below 1 σ (RMS beam size) [27,25].

- Bunch-by-bunch capabilities are required to perform measurements with high intensity beams by exciting a single bunch and measuring it for instance with all the BPMs (e.g. for coupling measurement).
- It is worth mentioning that recently a correlation between the temperature of the cryostat of a triplet and the beam orbit has been established: it is possible that the temperature variations that are usually observed also have an impact on the orbit of the beam, despite the low amplitude [70].
- It is also important to remember that a controlled longitudinal blow-up is performed during the ramp, which modifies the longitudinal phase space and the associated distributions: this could have some measurable impact in the transverse beam stability for some particular chromaticities [71].
- Finally, it is worth emphasizing that in the whole document the positions of the collimators are expressed in RMS beam sizes assuming a normalized transverse emittance of 2.5 μm (instead of the 3.5 μm used for the LHC).

In the following Tables the beam parameters at SPS extraction and the main HL-LHC nominal machine and beam parameters during the various phases of the cycle are provided (the crossing angle and separation offset refer to Beam 1 if not specified and B2 has always the opposite sign if not specified explicitly). The first three Tables are the same for both the nominal (levelling at a luminosity of 5×10^{34} $cm^{-2}s^{-1}$) and ultimate (levelling at a luminosity of 7.5×10^{34} $cm^{-2}s^{-1}$) scenarios:

- **Table 2**: Parameters at SPS extraction,
- **Table 3**: Parameters at the injection plateau after RF capture,
- **Table 4**: Parameters during ramp and squeeze.

The two following Tables are specific to the nominal scenario:

- **Table 5**: Parameters for the collision process (nominal),
- **Table 6**: Parameters in stable beams (nominal),

while the last three Tables concern the ultimate scenario:

- **Table 7**: Parameters during pre-squeeze (ultimate),
- **Table 8**: Parameters for the collision process (ultimate),
- **Table 9**: Parameters in stable beams (ultimate).

Table 2: Parameters at SPS extraction[1] [4]	HL-LHC (standard)	HL-LHC (BCMS)
Beam total energy [TeV]	0.45	
Particles per bunch, N [10^{11}]	2.3	
Maximum number of bunches	288	
ε_n [µm]	2.1 [72]	1.7
ε_L [eVs]	0.57	
RMS bunch length (q-Gaussian) [cm]	10.5	
RMS bunch length (FWHM equivalent Gaussian) [cm]	12.4	
FWHM bunch length [cm]	29.2	
RMS energy spread (q-Gaussian) [10^{-4}]	2.2	
RMS energy spread (FWHM equivalent Gaussian) [10^{-4}]	2.6	
FWHM energy spread [10^{-4}]	6.1	

[1] The Q20 optics is assumed, with a gamma transition of 17.951, 10 MV in the 200 MHz RF cavities and 1 MV in the 800 MHz RF cavities, in bunch shortening mode. The standard beam parameters are those requested by HL-LHC at injection and the BCMS beam emittance [3,72].

Table 3: Parameters at the injection plateau after RF capture	HL-LHC (standard)	HL-LHC (BCMS)
Beam total energy [TeV]	0.45	
Particles per bunch, N [10^{11}]	2.3	
Maximum number of bunches per beam	2760	2748
Filling pattern	standard[2]	BCMS[3]
ε_n (H,V) [μm] at start of injection plateau and before the ramp (with IBS, using Table 1)	Initial: 2.1, 2.1 Final: 2.3, 2.1	Initial: 1.7, 1.7 Final: 1.9, 1.7
Revolution frequency [kHz]	11.2455	
Harmonic number	35640	
RF frequency [MHz]	400.789	
Total RF voltage [MV]	8	
Length of the abort (no beam) gap [μs]	3	
Longitudinal beam loading compensation	Half detuning (i.e. no phase modulation)	
ε_L [eVs] at start of injection plateau and before the ramp (with IBS, using Table 1)	Initial: 0.57 Final: 0.63	Initial: 0.57 Final: 0.65
Synchrotron frequency [Hz]	66.0	
Bucket area [eVs]	1.38	
Bucket half height (ΔE/E) [10^{-4}]	9.65	
RMS bunch length (q-Gaussian) [cm] (with IBS, using Table 1)	7.8 to 8.3	7.8 to 8.4
RMS bunch length (FWHM equivalent Gaussian) [cm] (with IBS, using Table 1)	9.2 to 9.8	9.2 to 9.9
FWHM bunch length [cm] (with IBS, using Table 1)	21.7 to 23.1	21.7 to 23.3
RMS energy spread (q-Gaussian) [10^{-4}] (with IBS, using Table 1)	3.1 to 3.3	3.1 to 3.3
RMS energy spread (FWHM equivalent Gaussian) [10^{-4}] (with IBS, using Table 1)	3.6 to 3.9	3.6 to 3.9
FWHM energy spread [10^{-4}] (with IBS, using Table 1)	8.6 to 9.1	8.6 to 9.2
β^* [m] in IP1/2/5/8	6/10/6/10	
Optics	HLLHCV1.3 injection	
Tunes (H/V)	62.27/60.295	
Transition gamma (B1/B2)	53.8/53.9	
Half crossing angle at the IP for ATLAS (IP1) [μrad]	+295[4] (H[5])	
Half parallel separation at the IP for ATLAS (IP1) [mm]	+2.0[6] (V)	
Half external crossing angle at IP for ALICE (IP2) [μrad]	-170[6] (V)	
Half crossing angle at the IP for ALICE (IP2)[7] [μrad]	±1089 (V) -170 (V)	

[2] https://espace.cern.ch/HiLumi/WP2/Shared%20Documents/Filling%20Schemes%20HL-LHC/25ns_2760b_2748_2494_2572_288bpi_13inj.csv.

[3] https://espace.cern.ch/HiLumi/WP2/Shared%20Documents/Filling%20Schemes%20HL-LHC/25ns_2748b_2736_2258_2374_288bpi_12inj.csv.

[4] Compatible with DA studies done so far. Larger or smaller crossing angles could have some advantages but they would require further studies on beam-beam, field quality and energy deposition.

[5] In the horizontal plane there is no choice of sign as it is defined by the geometry.

[6] The other sign is possible and not correlated with other choices.

[7] The crossing angle in IP2 and IP8 is the sum of an external crossing angle bump and an "internal" spectrometer compensation bump (which is inversely proportional to the energy) and it depends on the spectrometer polarity. The values quoted above correspond to the sum of the two, noting that one configuration provides a minimum beam-beam long-range normalized separation. The external bump extends over the triplet and D1 and D2 magnets. The internal spectrometer compensation bump extends only over the long drift space between the two Q1 quadrupoles left and right from the IP. The convention for the spectrometer polarity sign is that it is positive for a

Half parallel separation at the IP for ALICE (IP2) [mm]	+3.5[8] (H)
External parallel angle at the IP for ALICE (IP2) [µrad]	-40[8] (H)
Angle at the IP for ALICE (IP2) [µrad]	-40 +/- 4.5 (B1H) 40 -/+ 4.5 (B2H)
Half crossing angle at the IP for CMS (IP5) [µrad]	+295[4,6] (V)
Half parallel separation at the IP for CMS (IP5) [mm]	-2.0[6] (H)
Half external crossing angle at the IP for LHCb (IP8) [µrad]	-170 (H)
Half crossing angle at the IP for LHCb (IP8)[7] [µrad]	±2100 (H) -170 (H)
Half parallel separation at IP for LHCb (IP8) [mm]	-3.5[8] (V)
External parallel angle at the IP for LHCb (IP8) [µrad]	-40[8] (V)
Angle at the IP for LHCb (IP8) [µrad]	-40 +/- 28 (B1V) 40 -/+ 28 (B2V)
Transverse damper damping time [turns]	10
Transverse damper bandwidth	Fully bunch-by-bunch
IBS growth-times (H,V,L) [h]	4.7, ∞, 3.5 | 3.0, ∞, 2.7
Damping times from synchrotron radiation (H,V,L) [10^3 h]	194.7, 194.7, 97.4
Power loss due to synchrotron radiation (W/m/beam)	~ 0
Chromaticity Q' (dQ/(dp/p))	+20[9]
Landau octupole Current (LOF) [A]	-40[9]
Collimators: TCP IR7 half-gap [σ]	6.7
Collimators: TCSG IR7 half-gap [σ]	7.9
Collimators: TCLA IR7 half-gap [σ]	11.8
Collimators: TCLD IR7 half-gap [σ]	20
Collimators: TCP IR3 half-gap [σ]	9.5
Collimators: TCSG IR3 half-gap [σ]	11.0
Collimators: TCLA IR3 half-gap [σ]	11.8
Collimators: TCSG IR6 half-gap [σ]	8.3
Collimators: TCDQ IR6 half-gap [σ]	9.5
Collimators: TCT IR1/5 half-gap [σ]	15.4
Collimators: TCL4-5-6 IR1/5 half-gap [mm]	25-25-25/25-25-25
Collimators: TCT IR2 half-gap [σ]	15.4
Collimators: TCT IR8 half-gap [σ]	15.4
Injection Protection: TDIS IR2 half-gap [mm]	3.9
Injection Protection: TDIS IR8 half-gap [mm]	3.8
Injection Protection: TCDD IR2 half-gap [mm]	24
Injection Protection: TCLIA IR2 half-gap [mm]	6.5
Injection Protection: TCLIA IR8 half-gap [mm]	6.6
Injection Protection: TCLIB IR2 half-gap [mm]	4.2
Injection Protection: TCLIB IR8 half-gap [mm]	2.8
Protected Aperture 1/5 [σ]	12.6
Crab Cavities: frequency [MHz]	400.789
Crab Cavities: voltage per cavity [MV]	0.25
Crab Cavities: phase between two cavities on the same IP side	±180

negative sign of the crossing angle (see http://lhc-beam-operation-committee.web.cern.ch/lhc-beam-operation-committee/documents/Xing/Spectrometers-help.ppt).

[8] The other sign is possible but the parallel angle and separation are correlated for the same IP.

[9] The scaling with intensity remains to be studied in detail but similar values were used until now for Run 2.

[deg]	
Crab Cavities: total voltage [MV]	0[10]
Crab Cavities: crabbing angle [μrad]	0
Crab Cavities: max. transverse emittance blow-up [μm/h]	≤ 0.04[11]

[10] As a result of the counter-phasing.

[11] It should be small with respect to the blow-up from IBS (of ~ 0.4 μm/h in H-plane), hence the factor 10. Due to the scaling discussed in Appendix B (in particular with respect to the β-function at the CC), this is believed to be realistic.

Table 4: Parameters during ramp and squeeze	HL-LHC (standard)	HL-LHC (BCMS)
Beam total energy [TeV]	0.45 to 7	
Particles per bunch, N [10^{11}]	2.3	
Maximum number of bunches per beam	2760	2748
Filling pattern	Standard[2]	BCMS[3]
ε_n (H,V) [µm]	2.3, 2.1	1.9, 1.7
Revolution frequency [kHz]	11.2455	
Harmonic number	35640	
RF frequency [MHz]	400.789 to 400.790	
Total RF voltage [MV]	8 to 16, linearly with time	
Length of the abort (no beam) gap [µs]	3	
Longitudinal beam loading compensation	Full detuning (with phase modulation)	
Peak-to-peak RF phase modulation[12][ps]	140 to 70	
ε_L [eVs]	0.63 to 3.03[13]	0.65 to 3.03[13]
Synchrotron frequency [Hz]	66.0 to 23.8	
Bucket area [eVs]	1.38 to 7.63	
Bucket half height (ΔE/E) [10^{-4}]	9.65 to 3.43	
RMS bunch length (q-Gaussian) [cm]	8.3 to 7.6	8.4 to 7.6
RMS bunch length (FWHM equivalent Gaussian) [cm]	9.8 to 9.0	9.9 to 9.0
FWHM bunch length [cm]	23.1 to 21.2	23.3 to 21.2
RMS energy spread (q-Gaussian) [10^{-4}]	3.3 to 1.1	3.3 to 1.1
RMS energy spread (FWHM equivalent Gaussian) [10^{-4}]	3.9 to 1.3	3.9 to 1.3
FWHM energy spread [10^{-4}]	9.1 to 3.0	9.2 to 3.0
β^* [m] in IP1/2/5/8	6/10/6/10 to 0.64[14]/10/0.64[14]/3	
Optics	HLLHCV1.3 injection to HLLHCV1.3 pre-squeeze (0.64 cm)	
Tunes (H/V)	62.27/60.295 to 62.31/60.32	
Transition gamma (B1/B2)	53.8/53.9 to 53.8/53.8	
Half crossing angle at the IP for ATLAS (IP1) [µrad]	+295[4] (H[5]) to +250[4] (H[5])	
Half parallel separation at the IP for ATLAS (IP1) [mm]	+2[6] to +0.55[6,15] (V)	
Half external crossing angle at IP for ALICE (IP2) [µrad]	-170[6] (V)	
Half crossing angle at the IP for ALICE (IP2)[7] [µrad]	±1089 (V) -170 (V) to ±70 (V) -170 (V)	
Half parallel separation at the IP for ALICE (IP2) [mm]	+3.5[8] to +1.4[8,15] (H)	
External parallel angle at the IP for ALICE (IP2) [µrad]	-40[8] to 0 (H)	
Angle at the IP for ALICE (IP2) [µrad]	-40 +/- 4.5 (B1H) to +/- 0.3 (B1H) 40 -/+ 4.5 (B2H) to -/+ 0.3 (B2H)	
Half crossing angle at the IP for CMS (IP5) [µrad]	+295[4,6] (V) to +250[4,6] (V)	
Half parallel separation at the IP for CMS (IP5) [mm]	-2[6] to -0.55[6,15] (H)	
Half external crossing angle at the IP for LHCb (IP8) [µrad]	-170 to -250 (H)	
Half crossing angle at the IP for LHCb (IP8)[7] [µrad]	±2100 (H) -170 (H) to ±135 (H) -250 (H)	

[12] The listed figures corresponds to a 3 µs long abort gap.

[13] With a controlled longitudinal blow-up.

[14] The limitation on β* at flat-top came from the sextupoles dI/dt in the 2017 Run. The exercise has to be redone with the final squeeze sequence, the circuit performance and the beam-beam considerations to establish the minimum β*.

[15] As currently used in the LHC. A further optimization for HL-LHC could be done if needed.

Half parallel separation at IP for LHCb (IP8) [mm]	-3.5[8] to -1.0[8,15] (V)	
External parallel angle at the IP for LHCb (IP8) [μrad]	-40[8] to 0 (V)	
Angle at the IP for LHCb (IP8) [μrad]	-40 +/- 28 (B1V) to +/- 1.8 (B1V) 40 -/+ 28 (B2V) to -/+ 1.8 (B2V)	
Transverse damper damping time [turns]	50	
Transverse damper bandwidth	Fully bunch-by-bunch	
IBS growth-times (H,V,L) [h]	β* = 6m: 5.8, ∞, 4.5 β* = 0.64 m: 15.3, ∞, 22.2	4.0, ∞, 3.7 10.9, ∞, 18.4
Damping times from synchrotron radiation (H,V,L) [10^3 h]	β* = 6m: 194.7, 194.7, 973.6 β* = 0.64 m: 0.052, 0.052, 0.026	
Power loss due to synchrotron radiation (W/m/beam)	~ 0 to 0.32	
Chromaticity Q' (dQ/(dp/p))	+20	
Landau octupole Current (LOF) [A]	-40 to < -300[16] scaling with ~ p^2	
Collimators: TCP IR7 half-gap [σ]	6.7	
Collimators: TCSG IR7 half-gap [σ]	7.9 to 9.1	
Collimators: TCLA IR7 half-gap [σ]	11.8 to 12.7[17]	
Collimators: TCLD IR7 half-gap [σ]	20 to 16.6	
Collimators: TCP IR3 half-gap [σ]	9.5 to 17.7	
Collimators: TCSG IR3 half-gap [σ]	11.0 to 21.3	
Collimators: TCLA IR3 half-gap [σ]	11.8 to 23.7	
Collimators: TCSG IR6 half-gap (B1/B2) [σ]	8.3 to 12.3 / 9.6	
Collimators: TCDQ IR6 half-gap (B1/B2) [σ]	8.3 to 12.3 / 9.6[18]	
Collimators: TCT IR1/5 half-gap [σ]	15.4 to 43.8	
Collimators: TCL4-5-6 IR1/5 half-gap [mm]	25-25-25/25-25-25	
Collimators: TCT IR2 half-gap [σ]	15.4 to 18.0	
Collimators: TCT IR8 half-gap [σ]	15.4 to 18.0	
Injection Protection: TDIS IR2 half-gap [mm]	55 (or 40[19])	
Injection Protection: TDIS IR8 half-gap [mm]	55 (or 40[19])	
Injection Protection: TCDD IR2 half-gap [mm]	42	
Injection Protection: TCLIA IR2 half-gap [mm]	29.5	
Injection Protection: TCLIA IR8 half-gap [mm]	28	
Injection Protection: TCLIB IR2 half-gap [mm]	28	
Injection Protection: TCLIB IR8 half-gap [mm]	28	
Protected Aperture 1/5 [σ]	12.6 to 19.4	
Crab Cavities: frequency [MHz]	400.789-400.790	
Crab Cavities: voltage per cavity [MV]	0.25	
Crab Cavities: phase between two cavities on the same IP side [deg]	±180	
Crab Cavities: total voltage [MV]	0[10]	
Crab Cavities: crabbing angle [μrad]	0	
Crab Cavities: max. transverse emittance blow-up [μm/h]	≤ 0.04[11]	

[16] 300 A (out of a maximum of 570 A) is the required current in the Landau octupoles to reach beam stability taking into account only the impedance model and without any margin (see Fig. 1).

[17] End point is under study for compatibility with TCDQ setting – see note below. This applies to the TCLA setting in all later Tables.

[18] This assumes that the TCDQ must stay constant in mm during the squeeze, with the mm point taken from the end of the squeeze at 15 cm, and the V1.3 optics as of 4/9/2017. It should be noted that the setting in mm is not compatible with the 5.2 mm TCDQ setting demanded by the ABT group, which means that the ABT requirements will have to be reviewed in the future or the optics redone. This note applies to the TCDQ setting in later configurations as well.

[19] We assume that we should be able to go to the fully-open position (55 mm) but, if we fall back in the same situation that we had in the past in IR8 (probably due to e-cloud), we might need to stay at 40 mm.

Table 5: Parameters for the collision process (nominal)	HL-LHC (standard)	HL-LHC (BCMS)
Beam total energy [TeV]	7	
Particles per bunch, N [10^{11}]	2.3	
Maximum number of bunches per beam	2760	2748
Number of colliding pairs in IP1/2/5/8 (at the end of the collision process)	2748/2494/2748/2572	2736/2258/2736/2374
Filling pattern	Standard[2]	BCMS[3]
Levelled pile-up in IP1/5/8	132/132/5.7	133/133/6.2
Levelled luminosity [10^{34} $cm^{-2}s^{-1}$] in IP1/2/5/8	5.0/0.001/5.0/0.2	5.0/0.001/5.0/0.2
ε_n [µm]	2.5	
Revolution frequency [kHz]	11.2455	
Harmonic number	35640	
RF frequency [MHz]	400.790	
Total RF voltage [MV]	16	
Length of the abort (no beam) gap [µs]	3	
Longitudinal beam loading compensation	Full detuning (with phase modulation)	
Peak-to-peak RF phase modulation[12] [ps]	70	
ε_L [eVs]	3.03	
Synchrotron frequency [Hz]	23.8	
Bucket area [eVs]	7.63	
Bucket half height ($\Delta E/E$) [10^{-4}]	3.43	
RMS bunch length (q-Gaussian) [cm]	7.6	
RMS bunch length (FWHM equivalent Gaussian) [cm]	9.0	
FWHM bunch length [cm]	21.2	
RMS energy spread (q-Gaussian) [10^{-4}]	1.1	
RMS energy spread (FWHM equivalent Gaussian) [10^{-4}]	1.3	
FWHM energy spread [10^{-4}]	3.0	
β^* [m] in IP1/2/5/8	0.64/10/0.64/3.0	
Optics	HLLHCV1.3 pre-squeeze (0.64 m)	
Tunes (H/V)	62.31/60.32	
Transition gamma (average B1/B2)	53.80	
Half crossing angle at the IP for ATLAS (IP1) [µrad]	+250[4] (H[5])	
Half parallel separation at the IP for ATLAS (IP1) [mm]	+0.55[6] to 0 (V)	
Half external crossing angle at IP for ALICE (IP2) [µrad]	-170[6] (V)	
Half crossing angle at the IP for ALICE (IP2)[7] [µrad]	±70 (V) -170 (V)	
Half parallel separation at the IP for ALICE (IP2) [mm]	+1.4[8] to + 0.138[8] (H) (see Appendix C)	
External parallel angle at the IP for ALICE (IP2) [µrad]	0 (H)	
Angle at the IP for ALICE (IP2) [µrad]	+/- 0.3 (B1H) -/+ 0.3 (B2H)	
Half crossing angle at the IP for CMS (IP5) [µrad]	+250[4,6] (V)	
Half parallel separation at the IP for CMS (IP5) [mm]	-0.55[6] to 0 (H)	
Half external crossing angle at the IP for LHCb (IP8) [µrad]	-250(H)	
Half crossing angle at the IP for LHCb (IP8)[7] [µrad]	±135 (H) -250 (H)	
Half parallel separation at IP for LHCb (IP8) [mm]	-1[8] to -0.043[8] (V) (see Appendix C)	
External parallel angle at the IP for LHCb (IP8) [µrad]	0 (V)	
Angle at the IP for LHCb (IP8) [µrad]	+/- 1.8 (B1V) -/+ 1.8 (B2V)	
Maximum total head-on tune shift	0.02	
Delay in the start of the collision process in IP1/2/5/8	Synchronised IP1 and IP5 to full head-on collision first, and then IP2 and IP8	
Time to go in collision in IP1/5 (from 2 σ full separation to 0 σ) [s]. No time constraint for IP2/8	< 3 [5, p.45]	
Transverse damper damping time [turns]	50	
Transverse damper bandwidth	Fully bunch-by-bunch	
IBS growth-times (H,V,L) [h]	24.7, ∞, 29.0	

Damping times from synchrotron radiation (H,V,L) [h]	51.7, 51.7, 25.9
Power loss due to synchrotron radiation (W/m/beam)	0.32
Chromaticity Q' (dQ/(dp/p))	+15
Landau octupole Current (LOF) [A]	< -300
Collimators: TCP IR7 half-gap [σ]	6.7
Collimators: TCSG IR7 half-gap [σ]	9.1
Collimators: TCLA IR7 half-gap [σ]	12.7
Collimators: TCLD IR7 half-gap [σ]	16.6
Collimators: TCP IR3 half-gap [σ]	17.7
Collimators: TCSG IR3 half-gap [σ]	21.3
Collimators: TCLA IR3 half-gap [σ]	23.7
Collimators: TCSG IR6 half-gap (B1 / B2) [σ]	12.3 / 9.6
Collimators: TCDQ IR6 half-gap (B1 / B2) [σ]	12.3 / 9.6
Collimators: TCT IR1/5 half-gap [σ]	18.0
Collimators: TCL4-5-6 IR1/5 half-gap [mm]	21.4-7.7-2.9/21.5-7.7-3.1
Collimators: TCT IR2 half-gap [σ]	43.8
Collimators: TCT IR8 half-gap [σ]	17.7
Injection Protection: TDIS IR2 half-gap [mm]	55 (or 40[19])
Injection Protection: TDIS IR8 half-gap [mm]	55 (or 40[19])
Injection Protection: TCDD IR2 half-gap [mm]	42
Injection Protection: TCLIA IR2 half-gap [mm]	29.5
Injection Protection: TCLIA IR8 half-gap [mm]	28
Injection Protection: TCLIB IR2 half-gap [mm]	28
Injection Protection: TCLIB IR8 half-gap [mm]	28
Protected Aperture 1/5 [σ]	19.4
Crab Cavities: frequency [MHz]	400.790
Crab Cavities: voltage per cavity [MV]	0.25 to 3.4[20]
Crab Cavities: phase between two cavities on the same IP side [deg]	±180 to 0
Crab Cavities: total voltage [MV]	0 to 6.8
Crab Cavities: crabbing angle [μrad]	0 to ± 180
Crab Cavities: max. transverse emittance blow-up [μm/h]	≤ 0.04[21]

[20] Before going in collision, we do the crabbing and then the collapse [73].

[21] Maximum acceptable transverse emittance blow-up to avoid less than ~ 1% of luminosity loss (see more explanation at the beginning of the note).

Table 6: Parameters in stable beams (nominal)	HL-LHC (standard)	HL-LHC (BCMS)
Beam total energy [TeV]	7	
Particles per bunch, N [10^{11}]	2.2 (start of fill)	
ε_n [µm]	2.5 (start of fill)	
Maximum number of bunches per beam	2760	2748
Number of colliding pairs in IP1/2/5/8	2748/2494/2748/2572	2736/2258/2736/2374
Filling pattern	Standard[2]	BCMS[3]
Levelled pile-up in IP1/5/8	131/131/5.6	132/132/6.1
Levelled luminosity [10^{34} $cm^{-2}s^{-1}$] in IP1/2/5/8	5.0/0.001/5.0/0.2	5.0/0.001/5.0/0.2
Levelling method in IP1/2/5/8	β^*/separation/β^*/separation	
Revolution frequency [kHz]	11.2455	
Harmonic number	35640	
RF frequency [MHz]	400.790	
Total RF voltage [MV]	16	
Length of the abort (no beam) gap [µs]	3	
Longitudinal beam loading compensation	Full detuning (with phase modulation)	
Peak-to-peak RF phase modulation[12] [ps]	70	
ε_L [eVs]	3.03 (start of fill)	
Synchrotron frequency [Hz]	23.8	
Bucket area [eVs]	7.63	
Bucket half height ($\Delta E/E$) [10^{-4}]	3.43	
RMS bunch length (q-Gaussian) [cm]	7.6 (start of fill)	
RMS bunch length (FWHM equivalent Gaussian) [cm]	9.0 (start of fill)	
FWHM bunch length [cm]	21.2 (start of fill)	
RMS energy spread (q-Gaussian) [10^{-4}]	1.1 (start of fill)	
RMS energy spread (FWHM equivalent Gaussian) [10^{-4}]	1.3 (start of fill)	
FWHM energy spread (FWHM equivalent Gaussian) [10^{-4}]	3.0 (start of fill)	
β^* [m] in IP1/2/5/8	0.64 to 0.15/10/0.64 to 0.15/3.0	
Optics	HLLHCV1.3 pre-squeeze (0.64 m) to HLLHCV1.3 pre-squeeze (0.50 m) to HLLHCV1.3 collision round (0.15 m)	
Tunes (H/V)	62.31/60.32	
Transition gamma (average B1/B2)	53.80 to 53.58	
Half crossing angle at the IP for ATLAS (IP1) [µrad]	+250[4] (H[5]) (norm. BBLR sep. from 21.8 σ to 10.5 σ)	
Half parallel separation at the IP for ATLAS (IP1) [mm]	0 (V)	
Half external crossing angle at IP for ALICE (IP2) [µrad]	-170[6] (V)	
Half crossing angle at the IP for ALICE (IP2)[7] [µrad]	±70 (V) -170 (V)	
Half parallel separation at the IP for ALICE (IP2) [mm]	+0.138[8] to 0 (H)	
External parallel angle at the IP for ALICE (IP2) [µrad]	0 (H)	
Angle at the IP for ALICE (IP2) [µrad]	+/- 0.3 (B1H) -/+ 0.3 (B2H)	
Half crossing angle at the IP for CMS (IP5) [µrad]	+250[4,6] (V) (norm. BBLR sep. from 21.8 σ to 10.5 σ)	
Half parallel separation at the IP for CMS (IP5) [mm]	0 (H)	
Half external crossing angle at the IP for LHCb (IP8) [µrad]	-250(H)	
Half crossing angle at the IP for LHCb (IP8)[7] [µrad]	±135 (H) -250 (H)	
Half parallel separation at IP for LHCb (IP8) [mm]	-0.043[8] to 0 (V)	
External parallel angle at the IP for LHCb (IP8) [µrad]	0 (V)	
Angle at the IP for LHCb (IP8) [µrad]	+/- 1.8 (B1V) -/+ 1.8 (B2V)	
Maximum total head-on tune shift	0.02	
Transverse damper damping time [turns]	50	
Transverse damper bandwidth	Standard (to reduce the associated noise)	
IBS growth-times (H,V,L) [h]	β^* = 0.64 m: 25.8, ∞, 30.3	

	β* = 0.15 m: 21.5, ∞, 33.7
Damping times from synchrotron radiation (H,V,L) [h]	β* = 0.64 m: 51.7, 51.7, 25.9 β* = 0.15 m: 51.7, 51.7, 25.9
Power loss due to synchrotron radiation (W/m/beam)	0.32 (at start of fill) and then decreases linearly with the total beam population
Chromaticity Q' (dQ/(dp/p)) for colliding bunches	+5
Landau octupole Current (LOF) [A] for colliding bunches	Any value should be possible for beam stability (tune spread dominated by BBHO) => To be optimised for DA
Chromaticity Q' (dQ/(dp/p)) for non-colliding bunches	+15
Landau octupole Current (LOF) [A] for non-colliding bunches	< -300
Collimators: TCP IR7 half-gap [σ]	6.7
Collimators: TCSG IR7 half-gap [σ]	9.1
Collimators: TCLA IR7 half-gap [σ]	12.7
Collimators: TCLD IR7 half-gap [σ]	16.6
Collimators: TCP IR3 half-gap [σ]	17.7
Collimators: TCSG IR3 [half-gap σ]	21.3
Collimators: TCLA IR3 half-gap [σ]	23.7
Collimators: TCSG IR6 half-gap (B1 / B2) [σ]	12.3 / 9.6 to 10.1
Collimators: TCDQ IR6 half-gap (B1 / B2) [σ]	12.3 / 9.6 to 10.1
Collimators: TCT half-gap IR1/5 [σ]	18.0 to 10.4[22]
Collimators: TCL4-5-6 IR1/5 half-gap [mm]	21.4-7.7-2.9/21.5-7.7-3.1
Collimators: TCT IR2 half-gap [σ]	43.8
Collimators: TCT IR8 half-gap [σ]	17.7
Injection Protection: TDIS IR2 half-gap [mm]	55 (or 40[19])
Injection Protection: TDIS IR8 half-gap [mm]	55 (or 40[19])
Injection Protection: TCDD IR2 half-gap [mm]	42
Injection Protection: TCLIA IR2 half-gap [mm]	29.5
Injection Protection: TCLIA IR8 half-gap [mm]	28
Injection Protection: TCLIB IR2 half-gap [mm]	28
Injection Protection: TCLIB IR8 half-gap [mm]	28
Protected Aperture 1/5 [σ]	19.4 to 11.9[22]
Crab Cavities: frequency [MHz]	400.790
Crab Cavities: voltage per cavity [MV]	3.4
Crab Cavities: phase between the two cavities on the same IP side [deg]	0
Crab Cavities: total voltage [MV]	6.8
Crab Cavities: crabbing angle [μrad]	±180 to ±190
Crab Cavities: max. transverse emittance blow-up [μm/h]	≤ 0.04[21]

[22] Relies on MKD-TCT phase advance being below 30 deg as obtained in the version 1.3 of the optics.

Table 7: Parameters during pre-squeeze (ultimate)	HL-LHC (standard)	HL-LHC (BCMS)
Beam total energy [TeV]	7	
Particles per bunch, N [10^{11}]	2.3	
Maximum number of bunches per beam	2760	2748
Filling pattern	Standard[2]	BCMS[3]
ε_n (H,V) [µm]	2.2, 2.0	1.9, 1.7
Revolution frequency [kHz]	11.2455	
Harmonic number	35640	
RF frequency [MHz]	400.790	
Total RF voltage [MV]	16	
Length of the abort (no beam) gap [µs]	3	
Longitudinal beam loading compensation	Full detuning (with phase modulation)	
Peak-to-peak RF phase modulation[12] [ps]	70	
ε_L [eVs]	3.03	
Synchrotron frequency [Hz]	23.8	
Bucket area [eVs]	7.63	
Bucket half height ($\Delta E/E$) [10^{-4}]	3.43	
RMS bunch length (q-Gaussian) [cm]	7.6	
RMS bunch length (FWHM equivalent Gaussian) [cm]	9.0	
FWHM bunch length [cm]	21.2	
RMS energy spread (q-Gaussian) [10^{-4}]	1.1	
RMS energy spread (FWHM equivalent Gaussian) [10^{-4}]	1.3	
FWHM energy spread [10^{-4}]	3.0	
β^* [m] in IP1/2/5/8	0.64/10/0.64/3.0 to 0.41/10/0.41/3.0	
Optics	HLLHCV1.3 end of ramp to pre-squeeze (0.50 m) and squeeze to 0.41 m	
Tunes (H/V)	62.31/60.32	
Transition gamma (average B1/B2)	53.86 to 53.80	
Half crossing angle at the IP for ATLAS (IP1) [µrad]	+250[4] (H[5])	
Half parallel separation at the IP for ATLAS (IP1) [mm]	+0.55[6] (V)	
Half external crossing angle at IP for ALICE (IP2) [µrad]	-170[6] (V)	
Half crossing angle at the IP for ALICE (IP2)[7] [µrad]	±70 (V) -170 (V)	
Half parallel separation at the IP for ALICE (IP2) [mm]	+1.4[8] (H)	
External parallel angle at the IP for ALICE (IP2) [µrad]	0 (H)	
Angle at the IP for ALICE (IP2) [µrad]	+/- 0.3 (B1H) -/+ 0.3 (B2H)	
Half crossing angle at the IP for CMS (IP5) [µrad]	+250[4,6] (V)	
Half parallel separation at the IP for CMS (IP5) [mm]	-0.55[6] (H)	
Half external crossing angle at the IP for LHCb (IP8) [µrad]	-250 (H)	
Half crossing angle at the IP for LHCb (IP8)[7] [µrad]	±135 (H) -250 (H)	
Half parallel separation at IP for LHCb (IP8) [mm]	-1.0[8] (V)	
External parallel angle at the IP for LHCb (IP8) [µrad]	0 (V)	
Angle at the IP for LHCb (IP8) [µrad]	+/- 1.8 (B1V) -/+ 1.8 (B2V)	
Transverse damper damping time [turns]	50	
Transverse damper bandwidth	Fully bunch-by-bunch	
IBS growth-times (H,V,L) [h]	β^* = 0.64 m: 15.3, ∞, 22.2 β^* = 0.41 m: 15.2, ∞, 22.3	10.9, ∞, 18.4 10.8, ∞, 18.4
Damping times from synchrotron radiation (H,V,L) [h]	β^* = 0.64 m: 51.7, 51.7, 25.9 β^* = 0.41 m: 51.7, 51.7, 25.9	
Power loss due to synchrotron radiation (W/m/beam)	0.32	
Chromaticity Q' (dQ/(dp/p))	+15	
Landau octupole Current (LOF) [A]	< -300	
Collimators: TCP IR7 half-gap [σ]	6.7	

Collimators: TCSG IR7 half-gap [σ]	9.1
Collimators: TCLA IR7 half-gap [σ]	12.7
Collimators: TCLD IR7 half-gap [σ]	16.6
Collimators: TCP IR3 half-gap [σ]	17.7
Collimators: TCSG IR3 half-gap [σ]	21.3
Collimators: TCLA IR3 half-gap [σ]	23.7
Collimators: TCSG IR6 half-gap (B1 / B2) [σ]	12.3 / 9.6 to 11.7 / 9.6
Collimators: TCDQ IR6 half-gap (B1 / B2) [σ]	12.3 / 9.6 to 11.7 / 9.6
Collimators: TCT IR1/5 half-gap [σ]	18.0 to 17.5
Collimators: TCL4-5-6 IR1/5 half-gap [mm]	25-25-25/25-25-25
Collimators: TCT IR2 half-gap [σ]	43.8
Collimators: TCT IR8 half-gap [σ]	17.7
Injection Protection: TDIS IR2 half-gap [mm]	55 (or 40^{19})
Injection Protection: TDIS IR8 half-gap [mm]	55 (or 40^{19})
Injection Protection: TCDD IR2 half-gap [mm]	42
Injection Protection: TCLIA IR2 half-gap [mm]	29.5
Injection Protection: TCLIA IR8 half-gap [mm]	28
Injection Protection: TCLIB IR2 half-gap [mm]	28
Injection Protection: TCLIB IR8 half-gap [mm]	28
Protected Aperture 1/5 [σ]	19.4 to 19.0
Crab Cavities: frequency [MHz]	400.790
Crab Cavities: voltage per cavity [MV]	0.25
Crab Cavities: phase between two cavities on the same IP side [deg]	± 180
Crab Cavities: total voltage [MV]	0^{10}
Crab Cavities: crabbing angle [μrad]	0
Crab Cavities: max. transverse emittance blow-up [μm/h]	$\leq 0.04^{21}$

Table 8: Parameters for the collision process (ultimate)	HL-LHC (standard)	HL-LHC (BCMS)
Beam total energy [TeV]	7	
Particles per bunch, N [10^{11}]	2.3	
Maximum number of bunches per beam	2760	2748
Number of colliding pairs in IP1/2/5/8 (at the end of the collision process)	2748/2494/2748/2572	2736/2258/2736/2374
Filling pattern	Standard[2]	BCMS[3]
Levelled pile-up in IP1/5/8	197/197/5.7	198/198/6.2
Levelled luminosity [10^{34} $cm^{-2}s^{-1}$] in IP1/2/5/8	7.5/0.001/7.5/0.2	7.5/0.001/7.5/0.2
ε_n [µm]	2.5	
Revolution frequency [kHz]	11.2455	
Harmonic number	35640	
RF frequency [MHz]	400.790	
Total RF voltage [MV]	16	
Length of the abort (no beam) gap [µs]	3	
Longitudinal beam loading compensation	Full detuning (with phase modulation)	
Peak-to-peak RF phase modulation[12] [ps]	70	
ε_L [eVs]	3.03	
Synchrotron frequency [Hz]	23.8	
Bucket area [eVs]	7.63	
Bucket half height ($\Delta E/E$) [10^{-4}]	3.43	
RMS bunch length (q-Gaussian) [cm]	7.6	
RMS bunch length (FWHM equivalent Gaussian) [cm]	9.0	
FWHM bunch length [cm]	21.2	
RMS energy spread (q-Gaussian) [10^{-4}]	1.1	
RMS energy spread (FWHM equivalent Gaussian) [10^{-4}]	1.3	
FWHM energy spread (FWHM equivalent Gaussian) [10^{-4}]	3.0	
β^* [m] in IP1/2/5/8	0.41/10/0.41/3.0	
Optics	HLLHCV1.3 squeeze (0.41 m)	
Tunes (H/V)	62.31/60.32	
Transition gamma (average B1/B2)	53.70	
Half crossing angle at the IP for ATLAS (IP1) [µrad]	+250[4] (H[5])	
Half parallel separation at the IP for ATLAS (IP1) [mm]	+0.55[6] to 0 (V)	
Half external crossing angle at IP for ALICE (IP2) [µrad]	-170[6] (V)	
Half crossing angle at the IP for ALICE (IP2)[7] [µrad]	±70 (V) -170 (V)	
Half parallel separation at the IP for ALICE (IP2) [mm]	+1.4[8] to +0.138[8] (H)	
External parallel angle at the IP for ALICE (IP2) [µrad]	0 (H)	
Angle at the IP for ALICE (IP2) [µrad]	+/- 0.3 (B1H) -/+ 0.3 (B2H)	
Half crossing angle at the IP for CMS (IP5) [µrad]	+250[4,6] (V)	
Half parallel separation at the IP for CMS (IP5) [mm]	-0.55[6] to 0 (H)	
Half external crossing angle at the IP for LHCb (IP8) [µrad]	-250(H)	
Half crossing angle at the IP for LHCb (IP8)[7] [µrad]	±135 (H) -250 (H)	
Half parallel separation at IP for LHCb (IP8) [mm]	-1.0[8] to -0.043[8] (V)	
External parallel angle at the IP for LHCb (IP8) [µrad]	0 (V)	
Angle at the IP for LHCb (IP8) [µrad]	+/- 1.8 (B1V) -/+ 1.8 (B2V)	
Maximum total head-on tune shift	0.02	
Delay in the start of the collision process in IP1/2/5/8	Synchronised IP1 and IP5 to full head-on collision first, and then IP2 and IP8	
Time to go in collision in IP1/5 (from 2 σ full separation to 0 σ) [s]. No time constraint for IP2/8	< 3 [5, p.45]	

Transverse damper damping time [turns]	50
Transverse damper bandwidth	Fully bunch-by-bunch
IBS growth-times (H,V,L) [h]	50.9, ∞, 43.7
Damping times from synchrotron radiation (H,V,L) [h]	51.7, 51.7, 25.9
Power loss due to synchrotron radiation (W/m/beam)	0.32
Chromaticity Q' (dQ/(dp/p))	+15
Landau octupole Current (LOF) [A]	< -300
Collimators: TCP IR7 half-gap [σ]	6.7
Collimators: TCSG IR7 half-gap [σ]	9.1
Collimators: TCLA IR7 half-gap [σ]	12.7
Collimators: TCLD IR7 half-gap [σ]	16.6
Collimators: TCP IR3 half-gap [σ]	17.7
Collimators: TCSG IR3 half-gap [σ]	21.3
Collimators: TCLA IR3 half-gap [σ]	23.7
Collimators: TCSG IR6 half-gap (B1 / B2) [σ]	11.7 / 9.6
Collimators: TCDQ IR6 half-gap (B1 / B2) [σ]	11.7 / 9.6
Collimators: TCT IR1/5 half-gap [σ]	17.5
Collimators: TCL4-5-6 IR1/5 half-gap [mm]	21.4-7.7-2.9/21.5-7.7-3.1
Collimators: TCT IR2 half-gap [σ]	43.8
Collimators: TCT IR8 half-gap [σ]	17.7
Injection Protection: TDIS IR2 half-gap [mm]	55 (or 40[19])
Injection Protection: TDIS IR8 half-gap [mm]	55 (or 40[19])
Injection Protection: TCDD IR2 half-gap [mm]	42
Injection Protection: TCLIA IR2 half-gap [mm]	29.5
Injection Protection: TCLIA IR8 half-gap [mm]	28
Injection Protection: TCLIB IR2 half-gap [mm]	28
Injection Protection: TCLIB IR8 half-gap [mm]	28
Protected Aperture 1/5 [σ]	19.0
Crab Cavities: frequency [MHz]	400.790
Crab Cavities: voltage per cavity [MV]	0.25 to 3.4
Crab Cavities: phase between the 2 cavities [deg]	±180 to 0
Crab Cavities: total voltage [MV]	0 to 6.8
Crab Cavities: crabbing angle [μrad]	0 to ±180
Crab Cavities: max. transverse emittance blow-up [μm/h]	≤ 0.04[21]

Table 9: Parameters in stable beams (ultimate)	HL-LHC (standard)	HL-LHC (BCMS)
Beam total energy [TeV]	7	
Particles per bunch, N [10^{11}]	2.2 (start of fill)	
ε_n [μm]	2.5 (start of fill)	
Maximum number of bunches per beam	2760	2748
Number of colliding pairs in IP1/2/5/8	2748/2494/2748/2572	2736/2258/2736/2374
Filling pattern	Standard[2]	BCMS[3]
Levelled pile-up in IP1/5/8	197/197/5.6	197/197/6.1
Levelled luminosity [10^{34} $cm^{-2}s^{-1}$] in IP1/2/5/8	7.5/0.001/7.5/0.2	7.5/0.001/7.5/0.2
Levelling method in IP1/2/5/8	β*/separation/β*/separation	
Revolution frequency [kHz]	11.2455	
Harmonic number	35640	
RF frequency [MHz]	400.790	
Total RF voltage [MV]	16	
Length of the abort (no beam) gap [μs]	3	
Longitudinal beam loading compensation	Full detuning (with phase modulation)	
Peak-to-peak RF phase modulation[12] [ps]	70	
ε_L [eVs]	3.03 (start of fill)	
Synchrotron frequency [Hz]	23.8	
Bucket area [eVs]	7.63	
Bucket half height (ΔE/E) [10^{-4}]	3.43	
RMS bunch length (q-Gaussian) [cm]	7.6 (start of fill)	
RMS bunch length (FWHM equivalent Gaussian) [cm]	9.0 (start of fill)	
FWHM bunch length [cm]	21.2 (start of fill)	
RMS energy spread (q-Gaussian) [10^{-4}]	1.1 (start of fill)	
RMS energy spread (FWHM equivalent Gaussian) [10^{-4}]	1.3 (start of fill)	
FWHM energy spread [10^{-4}]	3.0 (start of fill)	
β* [m] in IP1/2/5/8	0.41 to 0.15/10/0.41 to 0.15/3.0	
Optics	HLLHCV1.3 squeeze (0.41 m) to HLLHCV1.3 collision round (0.15 m)	
Tunes (H/V)	62.31/60.32	
Transition gamma (average B1/B2)	53.70 to 53.58	
Half crossing angle at the IP for ATLAS (IP1) [μrad]	+250[4] (H[5]) (norm. BBLR sep. from 17.3 σ to 10.5 σ)	
Half parallel separation at the IP for ATLAS (IP1) [mm]	0 (V)	
Half external crossing angle at IP for ALICE (IP2) [μrad]	-170 (V)	
Half crossing angle at the IP for ALICE (IP2)[7] [μrad]	±70 (V) -170 (V)	
Half parallel separation at the IP for ALICE (IP2) [mm]	+0.138[8] to 0 (H)	
External parallel angle at the IP for ALICE (IP2) [μrad]	0 (H)	
Angle at the IP for ALICE (IP2) [μrad]	+/- 0.3 (B1H) -/+ 0.3 (B2H)	
Half crossing angle at the IP for CMS (IP5) [μrad]	+250[4,6] (V) (norm. BBLR sep. from 17.3 σ to 10.5 σ)	
Half parallel separation at the IP for CMS (IP5) [mm]	0 (H)	
Half external crossing angle at the IP for LHCb (IP8) [μrad]	-250(H)	
Half crossing angle at the IP for LHCb (IP8)[7] [μrad]	±135 (H) -250 (H)	
Half parallel separation at IP for LHCb (IP8) [mm]	-0.043[8] to 0 (V)	
External parallel angle at the IP for LHCb (IP8) [μrad]	0 (V)	
Angle at the IP for LHCb (IP8) [μrad]	+/- 1.8 (B1V) -/+ 1.8 (B2V)	
Maximum total head-on tune shift	0.02	
Transverse damper damping time [turns]	50	
Transverse damper bandwidth	Standard (to reduce the associated noise)	
IBS growth-times (H,V,L) [h]	β* = 0.41 m: 25.6, ∞, 30.4 β* = 0.15 m: 21.5, ∞, 33.7	

Damping times from synchrotron radiation (H,V,L) [h]	β* = 0.41 m: 51.7, 51.7, 25.9 β* = 0.15 m: 51.7, 51.7, 25.9
Power loss due to synchrotron radiation (W/m/beam)	0.32 (at start of fill) and then decreases linearly with the total beam population
Chromaticity Q' (dQ/(dp/p)) for colliding bunches	+5
Landau octupole Current (LOF) [A] for colliding bunches	-100
Chromaticity Q' (dQ/(dp/p)) for non-colliding bunches	+15
Landau octupole Current (LOF) [A] for non-colliding bunches	< -300
Collimators: TCP IR7 half-gap [σ]	6.7
Collimators: TCSG IR7 half-gap [σ]	9.1
Collimators: TCLA IR7 half-gap [σ]	12.7
Collimators: TCLD IR7 half-gap [σ]	16.6
Collimators: TCP IR3 half-gap [σ]	17.7
Collimators: TCSG IR3 half-gap [σ]	21.3
Collimators: TCLA IR3 half-gap [σ]	23.7
Collimators: TCSG IR6 (B1 / B2) half-gap [σ]	11.7 / 9.6 to 10.1
Collimators: TCDQ IR6 (B1 / B2) half-gap [σ]	11.7 / 9.6 to 10.1
Collimators: TCT IR1/5 half-gap [σ]	17.5 to 10.4[22]
Collimators: TCL IR1/5 half-gap [mm]	21.4-7.7-2.9/21.5-7.7-3.1
Collimators: TCT IR2 half-gap [σ]	43.8
Collimators: TCT IR8 half-gap [σ]	17.7
Injection Protection: TDIS IR2 half-gap [mm]	55 (or 40[19])
Injection Protection: TDIS IR8 half-gap [mm]	55 (or 40[19])
Injection Protection: TCDD IR2 half-gap [mm]	42
Injection Protection: TCLIA IR2 half-gap [mm]	29.5
Injection Protection: TCLIA IR8 half-gap [mm]	28
Injection Protection: TCLIB IR2 half-gap [mm]	28
Injection Protection: TCLIB IR8 half-gap [mm]	28
Collimators: Protected Aperture 1/5 [σ]	19.0 to 11.9[22]
Injection Protection: TDIS IR2 half-gap [mm]	55
Crab Cavities: frequency [MHz]	400.790
Crab Cavities: voltage per cavity [MV]	3.4
Crab Cavities: phase between the 2 cavities [deg]	0
Crab Cavities: total voltage [MV]	6.8
Crab Cavities: crabbing angle [μrad]	±180 to ±190
Crab Cavities: max. transverse emittance blow-up [μm/h]	≤ 0.04[21]

The main plots for the baseline nominal and ultimate fill evolutions can be found in Fig. 4, assuming a constant crossing angle. For the nominal scenario, this would lead to a yearly-integrated luminosity of ~ 262 fb^{-1} for both standard and BCMS beams, assuming 160 days of operation, a turn-around time of 145 min (see Table 1) and an efficiency (defined as the time spent for successful fills [5]) of 50%. For the ultimate scenario, this would lead to a yearly-integrated luminosity of ~ 325 fb^{-1} for both standard and BCMS beams, assuming 160 days of operation, a turn-around time of 150 min (see Table 1) and an efficiency of 50%. With an efficiency of ~ 58% (as assumed in the past), ~ 370 fb^{-1}could be achieved per year. Note that the performance with the 8b+4e beam is ~ 25% lower [74]. However, there should be more margins with respect to beam-beam effects and a further optimization might be possible.

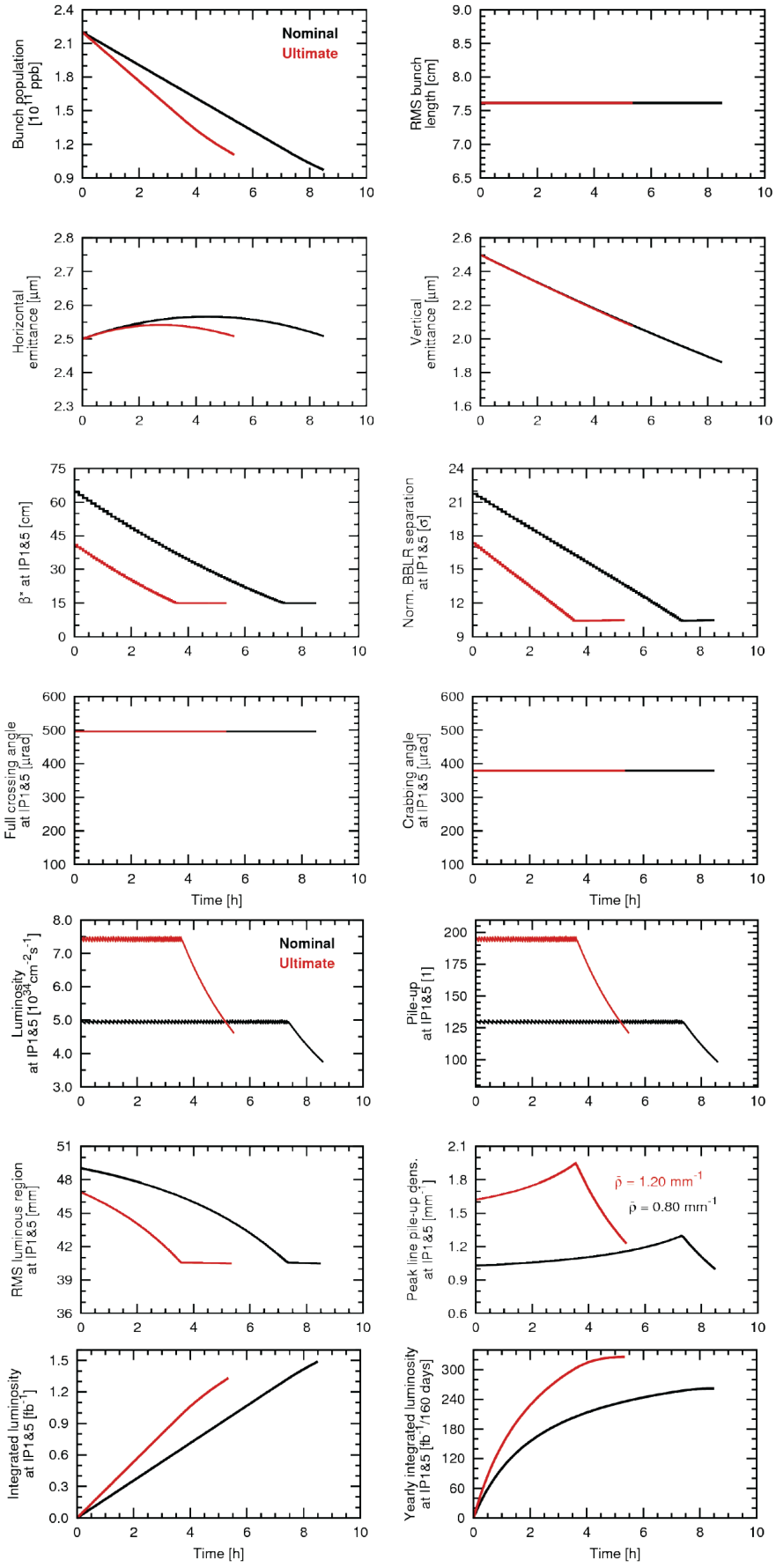

Figure 4: Main plots for the baseline nominal (and ultimate) fill evolutions assuming a constant crossing angle.

APPENDIX A: q-Gaussian longitudinal bunch profile

The longitudinal bunch profile in the LHC is well described at flat top (and it is also justified for HL-LHC) by

$$\lambda(s) = \frac{32}{5\pi S}\left(1 - \frac{4s^2}{S^2}\right), \quad |s| \le \frac{S}{2}.$$

This function is a particular case of the Tsallis q-Gaussian distribution [9]

$$f(s) = \frac{\sqrt{\beta}}{C_q}\mathrm{e}_q[-\beta(s-\mu)^2],$$

with mean $\mu = 0$, deformation parameter $q = 3/5$, and scale parameter $\beta = 10/S^2$. The normalization factor C_q and the q-exponential function in the equation above are given by

$$C_q = \begin{cases} \dfrac{2\sqrt{\pi}\,\Gamma\left(\frac{1}{1-q}\right)}{(3-q)\sqrt{1-q}\,\Gamma\left(\frac{3-q}{2(1-q)}\right)}, & -\infty < q < 1 \\ \sqrt{\pi}, & q = 1 \\ \dfrac{\sqrt{\pi}\,\Gamma\left(\frac{3-q}{2(1-q)}\right)}{\sqrt{q-1}\,\Gamma\left(\frac{1}{1-q}\right)}, & 1 < q < 3 \end{cases},$$

and

$$\mathrm{e}_q = \begin{cases} \exp(s), & q = 1 \\ [1+(1-q)s]^{\frac{1}{1-q}}, & q \neq 1 \text{ and } 1+(1-q)s > 0 \\ 0^{\frac{1}{1-q}}, & q \neq 1 \text{ and } 1+(1-q)s \le 0 \end{cases}.$$

Such a description is valid at the beginning of the fill, as the profile tends to Gaussian at the end of it. The RMS value of the q-Gaussian distribution $\lambda(s)$ is

$$\sigma_\lambda = \frac{S}{4\sqrt{2}}.$$

The q-Gaussian distribution is compared to the usual Gaussian description of the longitudinal bunch profile (characterized by the RMS bunch length σ) in Table 10. The relation between their corresponding RMS values is

$$\sigma_\lambda = \frac{\sigma}{2}\sqrt{\frac{\ln 2}{1-2^{-2/5}}} \approx 0.846\sigma.$$

For the Gaussian RMS bunch length of $\sigma = 9$ cm, $\sigma_\lambda = 7.6$ cm. With this, both distributions share an identical FWHM (21.2 cm), which is the parameter of interest for the threshold of the longitudinal beam stability [10].

Table 10: Comparison between the q-Gaussian distribution and the usual Gaussian description of the longitudinal bunch profile (with RMS bunch length σ).

	Gaussian	q-Gaussian
Distribution	$\rho(s) = \frac{1}{\sqrt{2\pi}\sigma}\exp\left(-\frac{s^2}{2\sigma^2}\right)$	$\lambda(s) = \frac{4\sqrt{2}}{5\pi\sigma_\lambda}\left(1-\frac{s^2}{8\sigma_\lambda^2}\right), \quad \lvert s\rvert \le 2\sqrt{2}\sigma_\lambda$
RMS	σ	σ_λ
FWHM	$\mathrm{FWHM}(\rho) = 2\sqrt{2\ln 2}\ \sigma$	$\mathrm{FWHM}(\lambda) = 4\sqrt{2}\sqrt{1-2^{-2/5}}\ \sigma_\lambda$

APPENDIX B: Transverse emittance growth from CCs

Without sophisticated feedback on the CC, but including the ADT damping effect, the currently estimated transverse emittance blow-up from the CCs is ~ 4.6%/h (at 7 TeV, β* = 15 cm and nominal CC voltage of 3.4 MV/CC), i.e. ~ 0.12 μm/h [75]. The absolute transverse emittance growth depends on both beam parameters and power spectral density of the RF noise on the betatron bands. Assuming constant betatron tune, RF noise spectrum and bunch length, the absolute growth rate of the normalized transverse emittance is i) proportional to the betatron function at the CC (inversely proportional to β*: at injection, the β-functions at the CCs are between 60 m and 290 m and at β* = 15 cm, they are between 2900 m and 4300 m), ii) proportional to the square of the CC voltage and iii) inversely proportional to the beam energy [76]. Some mitigation measures are currently under study (feedback on the CC voltage amplitude and phase from a measurement of the bunch transverse and head-tail motion) [77] and a factor 10 reduction of the growth rate is contemplated.

APPENDIX C: Levelling by transverse offset

IP2&8 will be levelled by parallel separation: Xip2 = 138 μm, which corresponds to 2.38 σ, and Yip8 = 43 μm, which corresponds to 1.36 σ. The luminosity reduction factor is plotted vs. the (full) transverse offset in Fig. 5.

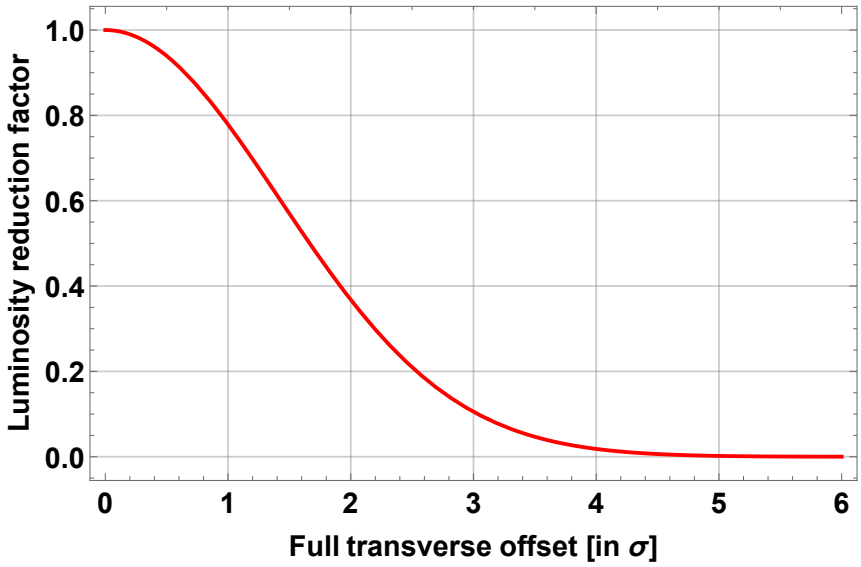

Figure 5: Luminosity reduction factor vs. the (full) transverse offset.

Acknowledgements

We would like to thank D. Banfi, O. Brüning, J. E. Müller, A. Valishev, A. Wolski and C. Schwick for their contributions to the definition of the machine and beam parameters.

References

[1] The ATLAS and CMS Collaborations, *Expected pile-up values at HL-LHC*, ATL-UPGRADE-PUB-2013-014, CERN (30 September 2013).

[2] D. Contardo, Private Communication, 03/12/2014.

[3] Métral, Elias, et al., *HL-LHC operational scenarios*, CERN-ACC-NOTE-2015-0009, 18/05/2015 (http://cds.cern.ch/record/2016811/files/CERN-ACC-NOTE-2015-0009_2.pdf).

[4] Métral, Elias, et al., *Update of the operational scenarios: stability vs. DA constraints*, 88th HiLumi WP2 Meeting, CERN, 21/03/2017 (https://indico.cern.ch/event/623917/contributions/2517809/attachments/1430972/2198219/Update_HLLHC-OPscenarios_21-03-2017.pdf).

[5] High-Luminosity Large Hadron Collider (HL-LHC). Technical Design Report V.0.1, edited by Apollinari G., Bejar Alonso I., Brüning O., Fessia P., Lamont M., Rossi L., Tavian L., CERN Yellow Reports: Monographs, Vol.4/2017, CERN-2017-007-M (CERN, Geneva, 2017). https://doi.org/10.23731/CYRM-2017-004.

[6] http://abpdata.web.cern.ch/abpdata/lhc_optics_web/www/hllhc13/.

[7] Métral, Elias, et al., *Transverse damping requirements*, 6th HL-LHC Collaboration Meeting, Paris, 15/11/2016 (https://indico.cern.ch/event/549979/contributions/2263239/attachments/1371420/2080427/TransverseDampingRequirements_EM.pdf).

[8] Shaposhnikova, Elena and Müller, Juan Esteban, *Bunch length and particle distribution for (HL-)LHC*, 82nd HiLumi WP2 Meeting, CERN, 12/01/2017 (https://indico.cern.ch/event/572439/contributions/2423329/attachments/1394442/2125205/HL-LHC_WP2_Jan17.pdf).

[9] Tomás Garcia, Rogelio and Medina, Luis, *Parameter update for the nominal HL-LHC: Standard, BCMS and 8b+4e*, 26th HL-LHC TCC, CERN, 16/03/2017 (https://indico.cern.ch/event/590415/contributions/2511517/attachments/1429118/2194441/2017-03-16_HLLHC-TC.pdf).

[10] Shaposhnikova, Elena and Müller, Juan Esteban, *Longitudinal stability limits and bunch length specifications*, 78th HiLumi WP2 Meeting, CERN, 23/09/2016 (https://indico.cern.ch/event/563288/contributions/2308739/attachments/1342048/2021482/HLLHC_WP2_v1.pdf).

[11] Redaelli, Stefano, *CONS and HL-LHC day 2017: Analysis of needs for LHC Collimation*

(https://indico.cern.ch/event/662417/contributions/2704978/attachments/1529943/2395488/SRedaelli_2017-09-26.pdf), presented during the "HL Consolidation Day", 26/09/2017 (https://indico.cern.ch/event/662417/).

[12] Buffat, Xavier et al., *Beam-beam effects in different luminosity levelling scenarios for the LHC*, Proc. of IPAC2014, Dresden, Germany (http://accelconf.web.cern.ch/AccelConf/IPAC2014/papers/tupro023.pdf?n=IPAC2014/papers/tupro023.pdf).

[13] Gorzawski, Arkadiusz Andrzej, *Luminosity control and beam orbit stability with beta star leveling at LHC and HL-LHC*, PHD thesis, EPFL, 2016 (https://infoscience.epfl.ch/record/222936/files/EPFL_TH7338.pdf).

[14] Fuchsberger, Kajetan et al., *β* leveling with telescopic ATS squeeze (MD 2410),* CERN-ACC-NOTE-2017-0052 (https://cds.cern.ch/record/2285184/files/CERN-ACC-NOTE-2017-0052.pdf).

[15] Bruce, Roderik, et al., *Protected aperture in HL-LHC*, 105th HiLumi WP2 Meeting, CERN, 26/09/2017 (https://indico.cern.ch/event/668031/contributions/2732276/attachments/1529772/2393803/2017.09.26--WP2_protected_aperture_v1.3_with_MKD_phase.pdf).

[16] Tsinganis, Andrea et al., *Impact of collision debris in the HL-LHC ATLAS and CMS insertions*, Proc. of IPAC2017, Copenhagen, Denmark (http://accelconf.web.cern.ch/AccelConf/ipac2017/papers/tupva021.pdf).

[17] Li, Kevin, et al., *Injection instabilities* (https://indico.cern.ch/event/589625/sessions/215347/attachments/1379237/2096177/02_IR_KL_new.pdf), presented during the "1/2-day internal review of LHC performance limitations (linked to transverse collective effects) during run II (2015-2016)", 29/11/2016 (https://indico.cern.ch/event/589625/).

[18] Persson, Tobias, et al., *Analysis of intensity-dependent effects on LHC transverse tunes at injection energy*, Proc. of IPAC2015, Richmond, VA, USA, 03-08/05/2015, (http://accelconf.web.cern.ch/AccelConf/IPAC2015/papers/tupty043.pdf).

[19] Ruggiero, Francesco, *Single-beam collective effects in the LHC*, CERN SL/95-09 (AP), LHC Note 313, 23/02/1995 (https://cds.cern.ch/record/279204/files/p83.pdf).

[20] Carver, Lee et al., *Destabilising effect of linear coupling in the LHC*, Proc. of IPAC2017, Copenhagen, Denmark (http://accelconf.web.cern.ch/AccelConf/ipac2017/papers/thpab040.pdf).

[21] *Review of the needs for a hollow e-lens for the HL-LHC*, CERN workshop, 06-07/10/2016 (https://indico.cern.ch/event/567839/).

[22] LHC Design Report, Vol I: the LHC Main Ring, edited by O. Brüning et al., CERN-2004-003-V-1 (https://cds.cern.ch/record/782076/files/CERN-2004-003-V1.pdf).

[23] Salvant, Benoit, et al., *Impedance and transverse beam stability for HL-LHC*, HL-LHC note under preparation. See also: Antipov, Sergey, et al., *Low-impedance collimators for HL-LHC*, ABP Group Information Meeting, CERN, 12/10/2017 (https://indico.cern.ch/event/671563/contributions/2749846/attachments/1539567/2413731/Coatings_in_Hi-Lumi_ABP_Info_Meeting_12.09.17_3.pdf).

[24] Antipov, Sergey et al., *HL-LHC Impedance model and stability*, 109th HiLumi WP2 meeting, CERN, 31/10/2017 (https://indico.cern.ch/event/674481/contributions/2769371/attachments/1549685/2434768/HL-LHC_Impedace_WP-2_31.10.17_2.pdf) and follow-up (https://indico.cern.ch/event/677574/contributions/2773932/attachments/1552137/2440615/Taking_a_closer_look_at_the_individual.pdf).

[25] Tambasco, Claudia, *Beam Transfer Function measurements and transverse beam stability studies for the Large Hadron Collider and its High Luminosity upgrade*, PHD thesis, EPFL, 2017, (https://infoscience.epfl.ch/record/230247/files/EPFL_TH7867.pdf).

[26] Fartoukh, Stéphane, *On the sign of the LHC octupoles*, CERN LMC meeting, 11/07/2012 (https://espace.cern.ch/lhc-machine-committee/Presentations/1/lmc_141/lmc_141h.pdf or https://cds.cern.ch/record/1972514/files/CERN-ACC-SLIDES-2014-0113.pptx).

[27] Buffat, Xavier, *Transverse beams stability studies at the Large Hadron Collider*, PHD thesis, EPFL, 2014, (https://infoscience.epfl.ch/record/204682/files/EPFL_TH6321.pdf).

[28] Buffat, Xavier et al., *Stability diagrams of colliding beams in the Large Hadron Collider*, PRST-AB 17, 111002 (2014), (https://cds.cern.ch/record/2011653/files/PhysRevSTAB.17.111002.pdf).

[29] Buffat, Xavier et al., *Update on the beam stability in the squeeze*, 110th HiLumi WP2 meeting, CERN, 07/11/2017 (https://indico.cern.ch/event/676590/contributions/2783107/attachments/1553707/2442289/2017-11-07_MadridPrep-expanded.pdf).

[30] Métral, Elias et al., *Stability diagram for Landau damping with a beam collimated at an arbitrary number of sigmas*, CERN-AB-2004-019-ABP (https://cds.cern.ch/record/733611/files/ab-2004-019.pdf).

[31] Fartoukh, Stéphane, *Breaching the Phase I optics limitations for the HL-LHC*, Proc. of the 2011 LHC Performance Workshop, Chamonix, 24-28/01/2011 (https://indico.cern.ch/event/103957/contributions/1301750/attachments/13636/19892/fartouk_upgrade.pdf).

[32] Fartoukh, Stéphane, *The Achromatic Telescopic Squeeze (ATS)*, 1st General HL-LHC meeting, CERN, 16-18/11/2011 (https://indico.cern.ch/event/150474/contributions/194167/attachments/153296/216944/fartouk_HLLHC.pdf).

[33] Fartoukh, Stéphane, *On the "LHC equation"*, CERN Beam-Beam and Luminosity Studies meeting, 16/06/2017 (https://indico.cern.ch/event/647249/contributions/2630436/attachments/1478211/2290837/LHCequation.pptx).

[34] Pellegrini, Dario *et al, Multiparametric response of the HL-LHC Dynamic Aperture in presence of beam-beam effects,* 2017 *J. Phys.: Conf. Ser.* **874** 012007 (http://iopscience.iop.org/article/10.1088/1742-6596/874/1/012007/pdf).

[35] Pieloni, Tatiana et al., *BBLR studies and possible reduction of the crossing angles in the LHC*, CERN LMC meeting, 31/08/2016 (https://espace.cern.ch/lhc-machine-committee/Presentations/1/lmc_275/CrossingAngle_Pieloni.pdf).

[36] Salvachua, Belen et al., *Observations of beam losses at the LHC during reduction of crossing angle*, Proc. of IPAC2017, Copenhagen, Denmark (http://accelconf.web.cern.ch/AccelConf/ipac2017/papers/tupva025.pdf).

[37] Crouch, Matthew et al., *Dynamic aperture studies of long-range beam-beam interactions at the LHC*, Proc. of IPAC2017, Copenhagen, Denmark (http://accelconf.web.cern.ch/AccelConf/ipac2017/papers/thpab056.pdf). See also Manchester University PHD thesis to be published.

[38] Pieloni, Tatiana et al., *Beam-beam effects long-range and head-on*, 6th Evian Workshop, 15-17/12/2015, Evian, France (https://indico.cern.ch/event/434129/contributions/1917209/attachments/1205686/1929911/EVIAN2015Pieloni.pdf).

[39] Pieloni, Tatiana et al., *Two beam effects*, Proc. of the 2014 Evian Workshop on LHC beam operation (https://cds.cern.ch/record/1968515/files/CERN-ACC-2014-0319.pdf).

[40] Banfi, Danilo et al., *Dynamic aperture studies with beam-beam, octupoles and chromaticity effects*, 46th CERN WP2 Task Leader Meeting, 10/04/2015 (https://indico.cern.ch/event/376194/contributions/889750/attachments/749816/1028676/DATL10_april_2015_ppt.pdf).

[41] Barranco, Javier et al., *Global compensation of long-range beam-beam effects with octupole magnets: dynamic aperture simulations for the HL-LHC case and possible usage in LHC and FCC*, CERN-ACC-NOTE-2017-036 (https://cds.cern.ch/record/2263347/files/CERN-ACC-NOTE-2017-0036.pdf).

[42] Barranco, Javier et al., *Study of beam-beam long range compensation with octupoles*, Proc. of IPAC2017 Copenhagen, Denmark (http://accelconf.web.cern.ch/AccelConf/ipac2017/papers/tupva027.pdf).

[43] Romano, Annalisa, et al., *Instabilities at stable beam* (https://indico.cern.ch/event/589625/sessions/215352/attachments/1379164/2095774/Internal_review_instability_stable_beamAR.pdf), presented during the "1/2-day internal review of LHC performance limitations (linked to transverse collective effects) during run II (2015-2016)", 29/11/2016 (https://indico.cern.ch/event/589625/).

[44] Romano, Annalisa, et al., *Stability with electron cloud*, 106th HiLumi WP2 meeting, CERN, 03/10/2017, (https://indico.cern.ch/event/668032/contributions/2737059/attachments/1533844/2401981/HLLHC_Meeting.pdf).

[45] Métral, Elias, et al., *Destabilising effect of the (resistive) transverse damper*, CERN LBOC meeting, 20/06/2017 (https://indico.cern.ch/event/647827/contributions/2633106/attachments/1479851/2294300/LBOC_EM_20-06-17.pdf).

[46] Oeftiger, Adrian, et al., *Can space charge stabilize head-tail instabilities at injection in the LHC?*, CERN LBOC meeting, 10/10/2017 (https://indico.cern.ch/event/672264/contributions/2750087/attachments/1538267/2411061/headtail_SC.pdf).

[47] Tomás Garcia, Rogelio, et al., *HL-LHC beam parameters for protons*, Proc. of the 2017 LHC Performance Workshop, 23-26/01/2017, Chamonix, France (https://indico.cern.ch/event/580313/contributions/2359501/attachments/1399837/2139071/SLIDESlogo.pdf).

[48] De Maria, Riccardo, et al., *What can be learnt in Run 2 for Run 3 and HL-LHC runs?*, Proc. of the 7th Evian Workshop, 13-15/12/2016, Evian, France (https://www.overleaf.com/read/zgxzhkwnqfrf#/29645255/).

[49] Rumolo, Giovanni, et al., *LIU baseline for protons*, Proc. of the 2017 LHC Performance Workshop, 23-26/01/2017, Chamonix, France (https://indico.cern.ch/event/580313/contributions/2359503/attachments/1401065/2160496/LIU-baseline-for-protons-2.pdf).

[50] Pellegrini, Dario, et al., *Scaling of DA with beam-beam effects (LR-HO): experience and simulations*, 79th HiLumi WP2 Meeting, CERN, 11/10/2016 (https://indico.cern.ch/event/563293/contributions/2316569/attachments/1352320/2041926/DA.pdf).

[51] Iadarola, Giovanni, et al., *Performance limitations from electron cloud in 2015*, Proc. of the 6th Evian Workshop, 15-17/12/2015, Evian, France (https://indico.cern.ch/event/434129/contributions/1917210/attachments/1205675/1837702/ecloud_evian2015.pdf).

[52] https://espace.cern.ch/HiLumi/WP2/Shared%20Documents/Filling%20Schemes%20HL-LHC/8b4e_1972b_1967_1178_1886_224bpi_12inj.csv. All the filling schemes (standard, BCMS and 8b+4e) can be found at https://espace.cern.ch/HiLumi/WP2/Wiki/HL-LHC%20Parameters.aspx.

[53] Bartosik, Hannes, et al., *MD421: Electron cloud studies on 25 ns beam variants (BCMS, 8b+4e)*, CERN-ACC-NOTE-2017-0028 (https://cds.cern.ch/record/2260998/files/CERN-ACC-NOTE-2017-0028.pdf).

[54] Stupakov, Gennady, *Decoherence of a Gaussian beam due to beam-beam interaction*, SSCL-Preprint-495, August 1993 (http://lss.fnal.gov/archive/other/ssc/sscl-preprint-495.pdf).

[55] Medina, Luis, and Tomás Garcia, Rogelio, *Follow up on the impact of crab cavity noise on luminosity*, 99th HiLumi WP2 Meeting, CERN, 25/07/2017 (https://indico.cern.ch/event/655317/contributions/2669001/attachments/1497988/2331941/2017-07-25_HLLHC-WP2.pdf).

[56] Karastathis, Nikos et al., *Emittance and lifetime evolution during 2017*, CERN LMC meeting, 04/10/2017 (https://indico.cern.ch/event/670908/contributions/2743826/attachments/1535110/2404543/emittance_LMC_04_10_2017_YP_final.pdf).

[57] Buffat, Xavier et al., *Observations of emittance growth in the presence of external noise in the LHC*, Proc. of IPAC2017, Copenhagen, Denmark (http://cds.cern.ch/record/2289677/files/tupva029.pdf).

[58] Baudrenghien, Philippe et al., *LHC full detuning (cavity phase modulation)*, CERN LBOC meeting, 11/04/2017 (https://indico.cern.ch/event/630941/contributions/2549763/attachments/1443317/2222891/FullDetuning.pdf).

[59] Mastoridis, Themis, et al., *Cavity voltage phase modulation to reduce the high-luminosity Large Hadron Collider rf power requirements*, PRAB, 20, 101003, 2017 (https://journals.aps.org/prab/pdf/10.1103/PhysRevAccelBeams.20.101003).

[60] Iadarola, Giovanni, et al., *Expected beam induced heat load on the beam screens*, 6th HL-LHC Collaboration Meeting, Paris, 15/11/2016 (https://indico.cern.ch/event/549979/contributions/2263201/attachments/1371446/2080455/012_gi_heat_loads_BS_paris.pdf).

[61] Iadarola, Giovanni et al., *Beam induced heat loads on HL-LHC Beam Screens*, 40th HL-LHC TCC meeting, CERN, 02/11/2017 (https://indico.cern.ch/event/676089/contributions/2767533/attachments/1551737/2438086/006_heat_load_overview_TCC.pdf).

[62] Baglin, Vincent, *HL-LHC vacuum system: base line, layout & aperture, material, RF bridges*, 97th HiLumi WP2 Meeting, CERN, 27/06/2017 (https://indico.cern.ch/event/647815/contributions/2633049/attachments/1483359/2301399/WP12_contribution_WP2_26_June_2017_VB_V2.pdf).

[63] Lamure, Anne-Laure, *Adsorption / Desorption from amorphous carbon coating at cryogenic temperature*, CERN TE-TM meeting, 05/10/2017 (https://indico.cern.ch/event/659343/contributions/2688555/attachments/1535604/2405442/LAMURE_TE-TM-PCh.pdf).

[64] Iadarola, Giovanni, et al., *Update on beam-induced heat load*, 106th HiLumi WP2 Meeting, CERN, 03/10/2017 (https://indico.cern.ch/event/668032/contributions/2737057/attachments/1533906/2402430/006_heat_load_update.pdf).

[65] Dijkstal, Philipp, et al., *Simulation studies on the electron cloud build-up in the elements of the LHC Arcs at 6.5 TeV*, CERN-ACC-NOTE-2017-0057 (https://cds.cern.ch/record/2289940/files/CERN-ACC-NOTE-2017-0057.pdf).

[66] Berkowitz Zamora, Daniel Alexander, *Update of cooling capacity and limitations*, 106th HiLumi WP2 Meeting, CERN, 03/10/2017 (https://indico.cern.ch/event/668032/contributions/2737058/attachments/1533950/2402612/2017-03-10_-_DBerkowitz_-_Summary_of_LOCAL_beam_screen_cooling_capacity_and_limitations_v1_1.pdf).

[67] Gonçalves Jorge, Patrik, *Observations and measurements of dynamic effects due to beam-beam interactions in the LHC and extrapolation to the FCC-hh*, EPFL Master thesis, CERN-THESIS-2017-161 (https://cds.cern.ch/record/2286079/files/CERN-THESIS-2017-161.pdf).

[68] Buffat, Xavier, et al., *Non-linear dynamic β effect*, 105th HiLumi WP2 Meeting, CERN, 26/09/2017 (https://indico.cern.ch/event/668031/contributions/2732274/attachments/1529761/2393753/2017-09-26_DynamicBeta-expanded.pdf).

[69] Wenninger, Jorg, et al., *Status of beta* levelling*, 104th HiLumi WP2 Meeting, CERN, 19/09/2017 (https://indico.cern.ch/event/666617/contributions/2724561/attachments/1524906/2385393/Leveling.HL-WP2.Sep17.pdf).

[70] Wenninger, Jorg, *Analysis of triplet movements*, CERN LBOC meeting, 24/10/2017 (https://indico.cern.ch/event/675411/contributions/2765003/attachments/1546063/2430787/TripletDrift-LBOC.Oct17.pdf).

[71] Oeftiger, Adrian, et al., *Transverse beam stability with realistic longitudinal profiles and contribution from space charge*, 109th HiLumi WP2 Meeting, CERN, 31/10/2017 (https://indico.cern.ch/event/674481/contributions/2769372/attachments/1549686/2434126/hllhc_headtails.pdf). See also https://indico.cern.ch/event/677574/contributions/2773932/attachments/1552137/2441613/DELPHI.pdf.

[72] Tomás Garcia, Rogelio et al., *HL-LHC beam parameters for protons*, Proc. of the 2017 LHC Performance Workshop, Chamonix, 23-27/01/2017 (https://indico.cern.ch/event/580313/contributions/2359501/attachments/1399837/2139071/SLIDESlogo.pdf).

[73] Tambasco, Claudia, et al., *Separation collapsing speed for HL-LHC*, 66th HiLumi WP2 Meeting, CERN, 19/04/2016 (https://indico.cern.ch/event/463032/contributions/1979649/attachments/1259995/1861804/HL_LHC_collapse_update.pdf).

[74] Medina, Luis, and Tomás Garcia, Rogelio, *Performance of the new baseline (and other operational scenarios)*, 108th HiLumi WP2 Meeting, CERN, 24/10/2017 (https://indico.cern.ch/event/668033/contributions/2759488/attachments/1546097/2426898/2017-10-24_HLLHC-WP2.pdf).

[75] Baudrenghien, Philippe, et al., *Crab cavities, RF noise and operational aspects (counter-phasing, full detuning). An update*, 96th HiLumi WP2

Meeting, CERN, 13/06/2017 (https://indico.cern.ch/event/645814/contributions/2622537/attachments/1475139/2291024/Meeting_13_06_2017.pdf).

[76] Baudrenghien, Philippe et al., *Transverse emittance growth due to rf noise in the high-luminosity LHC crab cavities*, PRST-AB, 18, 101001, 2015 (https://journals.aps.org/prab/pdf/10.1103/PhysRevSTAB.18.101001).

[77] Mastoridis, Themis, et al., *Noise mitigation by means of CC phase and amplitude feedback*, 101st HiLumi WP2 Meeting, CERN, 22/08/2017 (https://indico.cern.ch/event/659970/contributions/2692112/attachments/1510812/2355979/ABPtalk_Aug2017.pdf).